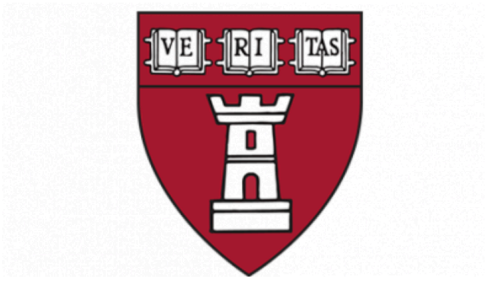

HARVARD UNIVERSITY
SCHOOL OF DENTAL MEDICINE

Requirement of Wnt Modulator *R-spondin3* in Craniofacial Morphogenesis and Dental Development

A Thesis Presented by

Nora Alhazmi, BDS, MS

To

The Faculty of Medicine
In partial Fulfillment of the Requirements for the Degree of
Doctor of Medical Sciences

Research Mentor:

Eric Chien-Wei Liao, MD, PhD

Associate Professor of Plastic and Reconstructive Surgery at Harvard Medical School

Harvard School of Dental Medicine
Boston, Massachusetts
April 2020

DEDICATION

This dissertation is dedicated to my dear parents "Nawal Alhawas and Zaid Alhazmi", my sister "Reem Alhazmi", my brothers "Fahad, Khalid and Ahmed Alhazmi" and my friends, for their unconditional love and support, throughout my journey

ACKNOWLEDGMENTS

First and foremost, I would like to express my sincere gratitude to my research mentor, Dr. Eric Chien-Wei Liao for his expertise, assistance and mentorship. I am grateful for his detailed guidance and encouragement throughout conducting this study for the past 2 years. He has been the best role model as a scientist, mentor and clinician.

Special thanks to our program director Dr. Francesca Gori for her scientific advice, knowledge and insightful contributions. In addition, I am thankful to the distinguished faculty members who served in my advisory and thesis committee: Dr. Roland Baron, Dr. Bjorn Olsen, Dr. Corneliu Sima, Dr. Yingzi Yang and Dr. Francesca Gori for their valuable time, insightful comments and knowledge.

I am thankful to Dr. Matthew Harris and Dr. Katherine Woronowicz for the micro CT images for adult zebrafish and their insightful comments. I am grateful to the postdoctoral research fellow Dr. Shannon H. Carroll for teaching and guiding me in the laboratory. Also, I am thankful to Dr. Liao's lab members in the Center for Regenerative Medicine department at Massachusetts General Hospital, for their help and support.

I would like to express my gratitude to my beloved country Saudi Arabia and King Saud bin Abdulaziz University for Health Sciences for sponsoring my postgraduate education.

Last but not least, I am thankful to my family; my parents "Nawal Alhawas and Zaid Alhazmi", my siblings "Reem, Fahad, Khalid and Ahmed Alhazmi" and my friends. Without their love, support and prayers it would have been more difficult to achieve my goals.

ABSTRACT

Wnt signaling plays a critical role in craniofacial, tooth and bone development. *Rspo3* is a key regulator of Wnt signaling; however, its function in craniofacial development and skeletogenesis is unknown. We show that *Rspo3* is expressed in perichondrial cells and osteoprogenitors in the developing embryonic palate and Meckel's cartilage in both zebrafish and mouse. In zebrafish, where tooth replacement is cyclic and occurs throughout the life of the animal, *rspo3* appears to be broadly expressed in the pulp, odontoblasts and epithelial crypts, and preferentially labels emerging teeth. Consistent with results obtained in the zebrafish, *Rspo3* is expressed in odontoblasts, pulp, ameloblasts and alveolar bone in the mouse. Using the zebrafish model, we show that *rspo3* disruption affects canonical Wnt signaling during embryogenesis. While mouse *Rspo3* global knockout is embryonic lethal, zebrafish *rspo3*-/- mutants are viable and show defects in the development of forming embryonic palate and in Meckel's cartilage morphology. Adult *rspo3*-/- mutant zebrafish exhibit decreased body length, hypodontia and abnormal dental morphology. Disruption of *rspo3* during zebrafish development resulted in poor ossification and dysmorphology of the adult zebrafish craniofacial skeleton and teeth. This study highlights the key functions of *Rspo3* in osteogenesis and morphogenesis of dentocranial structures.

Key words: wnt, *rspo3*, craniofacial, dental, bone, development

TABLE OF CONTENT

LIST OF FIGURES

LIST OF ABBREVIATION

aa: angularticular

BMD: bone mineral density

ch: ceratohyal

CL: cleft lip only

CL/P: cleft lip and/or palate

CNCCs: cranial neural crest cells

CPO: cleft palate only

d: dentary

dpf: days post-fertilization

e: eye

f: forebrain

fnp: frontonasal prominence

Grhl3: *Grainyhead-like 3*

hpf: hours post-fertilization

IACUC: Institutional Animal Care and Use Committee

IRF6: Interferon regulatory factor6

KLF4: *Krüppel-like factor 4*

m: Meckel's cartilage

mb: midbrain

MEE: medial edge epithelium

mnp: mandibular prominence

MO: morpholino

mxp: maxillary prominence

o: otic capsule

olf: olfactory placode

P: postnatal day

PPS: popliteal pterygium syndrome

Rspo: *R-spondin*

S: stomodeum

t: trabecula

tel: telencephalon

TGF: Transforming growth factor

TRAP: Tartrate-resistant acid phosphatase

TSR1: thrombospondin type 1 repeat

VWS: Van der Woude syndrome

WGS: Whole-genome sequencing

WISH: whole-mount RNA *in situ* hybridization

WT: wild type

y: yolk sac

zfin: Zebrafish Information Network

LIST OF SYMBOLS

μm: micrometer

μ: micron

R^2: coefficient of determination

RFU: relative fluorescence units

“Requirement of Wnt Modulator *R-spondin3* in Craniofacial Morphogenesis and Dental Development”

INTRODUCTION

Craniofacial growth and development:

Understanding craniofacial growth and development is more than a scientific curiosity, it is of tremendous interest to clinicians and the general community.[1] Mechanistic insight into craniofacial development is important in order to improve diagnosis and treatment for patients with dentofacial deformities and craniofacial anomalies, such as cleft lip and palate and craniosynostosis.[1] Observational studies have been carried out to understand prenatal and postnatal craniofacial growth.[1] However, gaps of knowledge remain in areas of macroscopic growth and cells, genes and matrix molecules that are responsible for craniofacial growth.[1]

Growth is defined as an increase in cells number and size and it is controlled by intrinsic genetic, epigenetic and environmental factors.[1,2] On the other hand, development refers to growth and maturation encompassing morphogenesis, differentiation and function.[2] Cranial neural crest cells specification, migration, proliferation and ultimate fate determination play an important feature in craniofacial development.[3] Craniofacial development is initiated by the ventrolateral migration of cranial neural crest cells from the dorsal neural tube to create the ectomesenchyme of the frontonasal prominence and pharyngeal arches.[4,5] The frontonasal prominence is derived from the midline primordium and contributes to the formation of the forehead, philtrum of the upper lip and primary palate.[6,7] The first pharyngeal arch appears as small swelling that further divides into the maxillary and mandibular components.[3,8] The maxillary prominence forms the lips and secondary palate, and the lower jaw develops from the mandibular prominence.[7] This early pharyngeal arch patterning is conserved across vertebrates which justifies the use of mouse and zebrafish models to understand human craniofacial development (Fig. 1).[9]

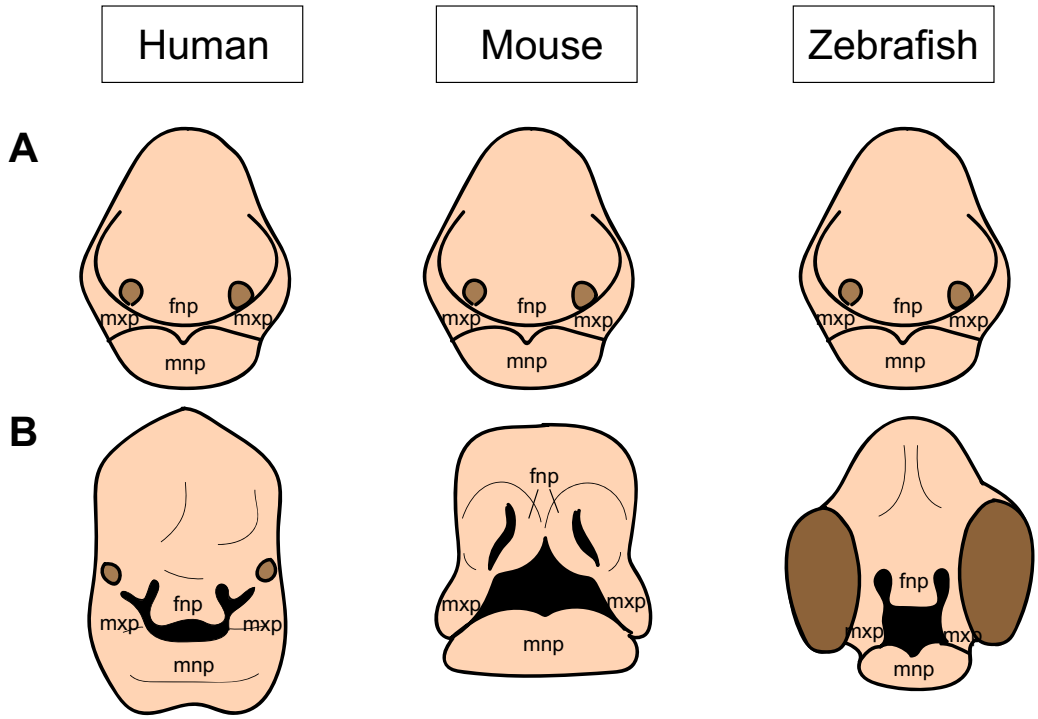

Fig. 1. Diagram illustrating the conserved pharyngeal arch patterning across vertebrates. A) early pharyngeal arch patterning is conserved across vertebrates. B) Later development of human, mouse and zebrafish embryos showing the development of the face. Abbreviations: fnp: frontonasal prominence, mxp: maxillary prominence, mnp: mandibular prominence

In zebrafish, the ethmoid plate originates from cranial neural crest to form the roof of the mouth/cranial base and is derived from convergence of three distinct parts: the frontonasal median element derived from the most anterior stream of migrating cranial neural crest cells (CNCCs), and paired maxillary elements derived from the second stream of CNCCs.[10,11] In this way, the zebrafish ethmoid plate (hereafter palate) is analogous to mammalian palate (Fig. 2).[12] In this study, we used mouse and zebrafish models. The mouse model has the advantage of resembling mammalian morphogenesis and has powerful genetics.[13] However, the zebrafish system has the advantages of transparent embryos, rapid and external development and is suitable for high resolution imaging.[12]

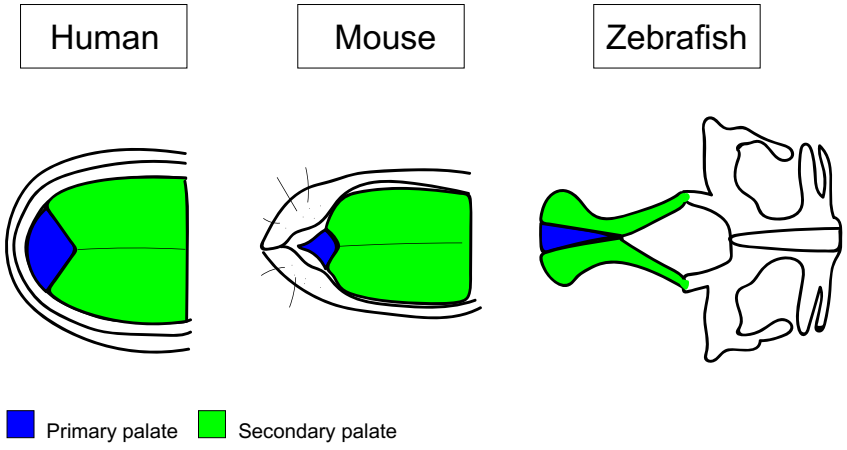

Fig. 2. Diagram illustrating the zebrafish model of mammalian hard palate. This figure shows primary palate (blue) and secondary palate (green) in human, mouse and zebrafish.

Cleft lip and palate origin, prevalence and genetic etiology:

Orofacial clefts are one of the most common congenital birth anomalies in humans, affecting 1 in 700 live births.[14] Orofacial clefts can present in a spectrum of clinical phenotypes; cleft lip and/or palate (CL/P), cleft lip only (CL) or cleft palate only (CPO) with strong genetic predisposition that is influenced by environmental factors and epigenetics.[15,16,17]

The treatment of CL/P requires a multidisciplinary team of health care providers including pediatrician, surgeon, otolaryngologist, orthodontist, speech therapist, psychologist, geneticist and social worker to guide and identify every aspect of the child's care.[18] The clinical treatment involves multiple procedures that follows a specific timeline starting from surgically repairing of cleft lip at 3 to 5 months of age followed by cleft palate repair at 6 to 18 months and ENT therapy.[18] Speech therapy and dental care begins at 2 years of age with regular follow up visits. Moreover, orthodontic treatment is required around 7 to 10 years of age for alveolar bone grafting and alignment of teeth and orthognathic surgery is sometimes needed at the completion of growth, around 21 years of age. The complex management of CL/P also requires coordinated longitudinal care. This starts with identification of the malformation at screening

prenatal ultrasound, and is followed by educating and preparing the parents regarding feeding, to age of mixed dentition with bone grafts and subsequent orthodontic management, until late teens which involve revision rhinoplasty and perhaps orthognathic surgery.[18] Orofacial clefts and their treatment incur social and psychological burdens, as well as financial burden to the patients and their families because of the long-term treatment costs and the multidisciplinary treatment. The ultimate goal of this research is to understand the pathogenesis of CL/P and their preventive therapeutics such as the dramatic effects of folate prenatal supplement on spina bifida incidence.

There are multiple genes and genetic pathways that contribute to craniofacial development.[19] For example, *Interferon regulatory factor6 (IRF6)* belongs to a family of nine transcription factors which share a highly conserved winged-helix DNA binding domain and is expressed in the ectoderm of palatal shelves during the development of secondary palate.[20,21] Mutation of *IRF6* plays a significant role in cleft pathogenesis, accounting for approximately 12% of cases.[22,23] *IRF6* has been linked to CLP syndromes (popliteal pterygium syndrome (PPS) and Van der Woude syndrome (VWS)) as well as non-syndromic CL/P.[21,24] *Irf6* is highly conserved across different species with 80% identity in DNA binding and protein-binding domains.[21,25] *Pbx-Wnt-p63* pathway has been reported to regulate the expression of *Irf6* during face morphogenesis.[26] In addition, *Transforming growth factor (TGF*) signaling mediates *Irf6* expression and regulates medial edge epithelium (MEE) degeneration during palatal fusion in mice experiments.[27] In this study, we investigated the role of *Irf6* and its downstream targets in cleft lip and palate pathogenesis.

The important role of Wnt/β-catenin signaling in craniofacial development and skeletal patterning:

Wnt/β-catenin signaling is necessary for the generation, migration and survival of cranial neural crest cells during craniofacial development.[28,29] Wnt proteins are highly conserved across vertebrates and plays an important role in patterning and morphogenesis.[30] Canonical signaling is strongly expressed in the first pharyngeal arch as well as multiple craniofacial regions in mouse, chicken and zebrafish during embryogenesis.[31-34] In addition, Wnt signaling plays a role in mediating regional specification in the vertebrate face.[6] Mutation in *WNT3* gene is associated with cleft lip and palate in human.[35] Furthermore, central nervous system defects and absences of craniofacial development has been reported in β-catenin mutant mice embryos.[29]

Besides Wnt/β-catenin signaling role in craniofacial development, it plays a major role in skeletal patterning and differentiation during embryonic development, and in maintaining postnatal bone homeostasis.[36-38] Wnt signaling is involved in regulating skeletogenic neural crest cells, such as the subdivision of each pharyngeal arch into dorsal and ventral elements in zebrafish during craniofacial development.[10] Impairment and potentiation of Wnt signaling affects overall bone mass and density in human.[36-38] The canonical β-catenin mediated Wnt signaling pathway directly regulates osteoblast differentiation and activity and likely has an indirect effect on osteoclasts during bone metabolism.[39] Moreover, direct negative influence of canonical Wnt/β-catenin signaling on osteoclasts development in cell lines and mouse models have been reported.[40] Identification of modulators of Wnt signaling during craniofacial development and homeostasis of adult skeletal tissues may lead to new insights into disease etiology and inroads for therapeutic mediation.

The role of *R-spondins* in embryogenesis and skeletal development:

The *R-spondin* (*Rspo*) family of secreted proteins includes four members (*Rspo1* to *4*) in the thrombospondin type 1 repeat (TSR1)-containing protein superfamily and have been shown to potentiate canonical Wnt/β-catenin pathway.[41,42] *Rspo* proteins modulate Wnt signaling through interaction with the Wnt receptor complex, including LGR4/5/6, that leads to stabilization of Frizzled and LRP*5/6* at the cell membrane, and regulation of the ubiquitin ligases ZNFR3 and RNF43 that degrade Frizzled receptor (Fig. 3).[43-45]

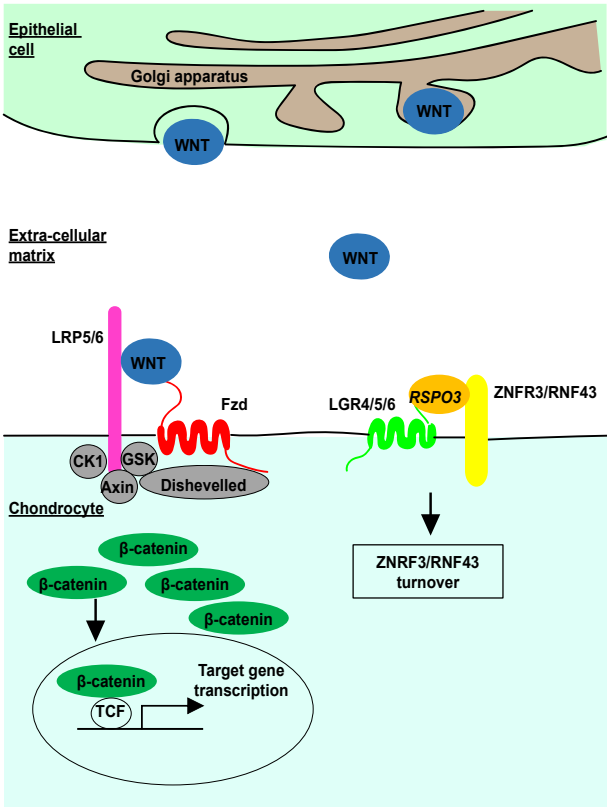

Fig. 3. Schematic diagram showing RSPO3 augmentation of Wnt/β-catenin signaling. Binding of RSPO3 to LGR5/6 causes clearance of ZNRF3/RNF43 from the membrane which results in stabilization of LRF5/6 and Frizzled in the plasma membrane. Therefore, RSPO3 binding results in potentiation of Wnt/β-catenin signaling.

Rspo2 and Rspo3 proteins have also been shown to also potentiate Wnt/β-catenin signaling by binding to heparin sulfate proteoglycans to localize them in the intercellular

space.[43-45] In addition, *Rspos* are involved in embryonic differentiation and patterning.[46,47] *Rspo1* plays a role during the development of reproductive organs and skin maturation and *Rspo4* functions as a key regulator of nail development.[48,49] Human *RSPO4* mutations has been linked to total or partial absence of fingernails.[50] *Rspo2* and *Rspo3* have been reported to be more potent in Wnt signaling activation and stabilization compared to *Rspo1* and *Rspo4*.[51] *Rspo2* is expressed and function in the first pharyngeal arch morphogenesis by ectodermal-mesenchymal interaction.[52] Recessive *RSPO2* mutations in human causes tetra-amelia syndrome that is characterized by lung aplasia, total absences of the four limbs and cleft lip and palate.[53] In addition, *Rspo2* knockout mice showed limb malformation, lung hypoplasia and cleft palate phenotype.[54,55] Jin et al. reported that the mandibular hypoplasia and insufficient tongue space in *Rspo2* null mouse could be the cause of CPO due to failure of palatal shelves elevation during development.[52]

Rspo3 was identified in 1971 as a thrombin sensitive protein.[56] *Rspo3* overall sequence identity between zebrafish and human is 45%.[57] Human *RSPO3* was identified as a candidate gene for cleft lip/palate and dental anomalies.[58] *Rspo3* has a critical role in mouse placental development.[59] Mice embryos lacking *Rspo3* function die at E10.5 due to placenta and vascular defects.[59,60] Therefore, conditional ablation of *Rspo3* via Cre recombinase expression is necessary to investigate *Rspo3* function beyond E10.5.[61] Severe hindlimb truncations were found in *Prx1-cre* conditional *Rspo3* and *Rspo2* mutant mice.[61] *Rspo3* plays a role in early hematopoietic cell specification, cell proliferation, vascular morphogenesis and remodeling in *Xenopus* embryos.[60] Knockdown of *rspo3* in Xenopus using morpholino injection caused ventral edema due to vascular defects.[60] Moreover, *Rspo3* is required for *Vegf* expression in Xenopus and mouse embryos.[60] *rspo3* is also required for the morphogenesis of head cartilage

in Xenopus embryos.[62] Despite these findings, the full function of *Rspo3* during embryogenesis requires further elucidation.[63]

Human genome wide association studies have implicated many regulators of canonical Wnt signaling pathway in the regulation of bone metabolism.[64] *RSPO2* and *RSPO3* have been associated with human bone mineral density.[64-66] For example, osteoporosis is characterized with low bone mineral density and increase risk for bone fracture and *RSPO3* gene has been reported to affects bone mass regulation in early adulthood.[64] Therefore, *RSPO3* is used as a genetic marker for bone mass and fracture risk in human since it affects bone mass regulation in early adulthood.[65,67] In mice, deletion of *Rspo* receptor LGR4 leads to reduced bone mass due to decreased bone formation and increased bone resorption suggesting the role of Rspo in bone maintenance.[68] *Rspos* are essential for normal development and have been shown to regulate skeletal pattern during development.[61] In particular, *RSPO2* deletion mutations has been identified in fetuses presented with sever limb defects.[53] Moreover, *Rspo2* has been shown to be essential for mice limb patterning in concert with *Rspo3*.[61] *Rspo3* is expressed in the mesenchymal cells of limb bud at E10.5 in mice.[69,70] In addition, *Rspo2* and *Rspo3* have an important role in limb elongation and formation of distal structures.[69,70] In summary, *Rspos* have an important role the development and maintenance of bones.[69,70]

<u>*Rspo3* is a transcriptional target of *irf6*:</u>

Since CL/P has a fundamental genetic basis where *IRF6* is a key genetic determinant, identification of *IRF6* target genes have led to additional CL/P determinants such as *Grainyhead-like 3* (*Grhl3*) and *Krüppel-like factor 4* (*KLF4*).[71] Our lab carried out comparative ChIP-seq and RNA-seq experiments using wildtype and maternal-null *irf6* mutants zebrafish

embryos at 5 hours post-fertilization (hpf) in order to identify downstream *irf6* transcriptional target genes. The ChIP-seq results showed *irf6* binding peaks representing 2,201 genes and the RNA-seq revealed significant downregulation of genes with disruption of *irf6* function. From the overlap of mRNA-seq and ChIP-seq results, a dataset of 320 genes were identified. To narrow down the *irf6* candidate genes, this dataset was further refined to 277 genes that have strong cross-species conservation of DNA and protein sequences. Thereafter, these genes were integrated with FaceBase data on mouse embryonic facial prominence gene expression to identify genes with relevant craniofacial expression patterns and this narrow the list to 271 candidate genes. Finally, 18 candidate genes were selected after review of published literature, examination of the mouse Gene Expression Database and Zebrafish Information Network (zfin). From these 18 candidate genes, *rspo3* was identified as a *irf6* target gene (Fig. 4).

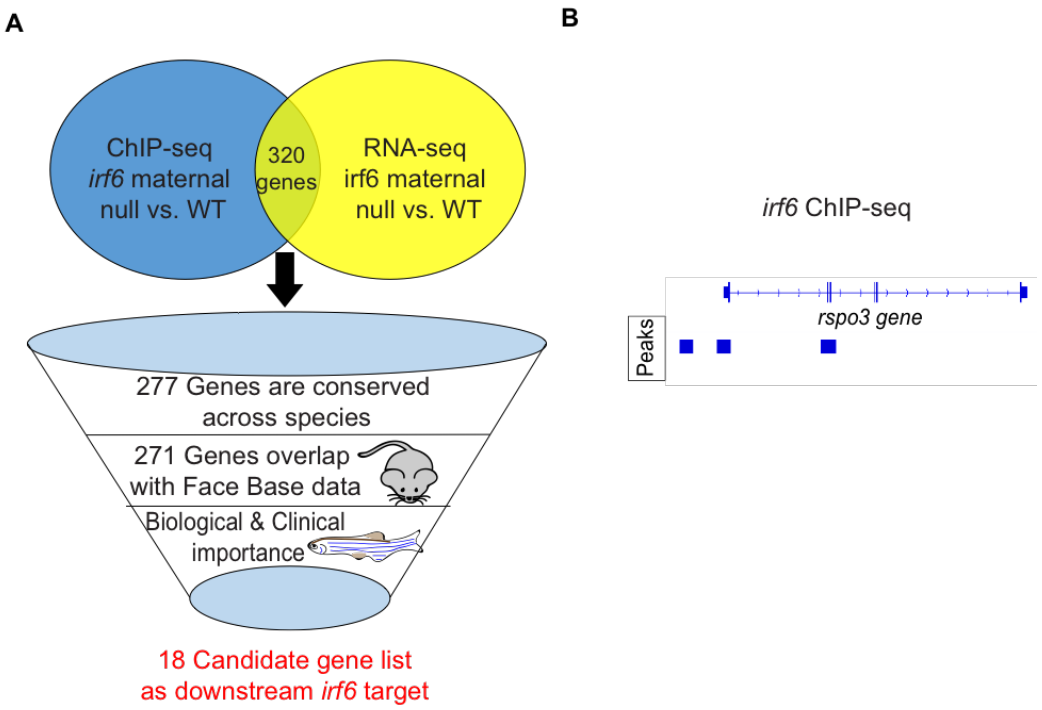

Fig. 4. *rspo3* is a transcriptional target of *irf6*. A) We performed ChIP-seq and RNA-seq datasets on *irf6* mutant zebrafish embryos and wild type. In order to narrow the downstream target genes of *irf6*, we integrated ChIP-seq and RNA-seq dataset with mouse gene expression datasets from FaceBase. Based on the biological, clinical importance and integrated data, we

found 18 candidate gene for *irf6* and *rspo3* is one of these candidate genes. B) *irf6* ChIP-seq reads demonstrating peaks directly overlying the upstream of *rspo3* as well as the transcriptional site.

The role of Wnt signaling in dental morphogenesis:

Wnt/β-catenin pathway also plays a critical role in tooth development and can affect craniofacial development more broadly.[72] Tooth formation initiates from the interactions between the epithelial layer and the underlying mesenchyme structure.[73,74] Vertebrates share some features of dental development such as formation of epithelial bud, mesenchymal condensation and deposition of mineralizing matrices.[75-77] However, some vertebrates differ in tooth attachment, dental eruption and in enamel production.[75-77] Humans develop two sets of teeth; 20 primary teeth and 32 permanent teeth with no replacement.[78] Mice have a single set of dentition that consists of one incisor and three molars in single row in both sides of upper and lower jaws with no replacement.[79,80] However, rodent incisors undergoes continuous regeneration from the stem cells located in the proximal side.[81] Unlike human and mouse tooth development, zebrafish dentition is more numerous and show continuous replacement.[82] In addition, zebrafish have no oral teeth.[76] Teeth are attached to pharyngeal jaws.[76] Moreover, there are three rows of teeth on each side consisting of ventral row of five teeth, mediodorsal row of four teeth and a dorsal row of two teeth.[83] Despite these differences, the development of zebrafish primary and replacement teeth are similar to mammalian teeth (Fig. 5).[82]

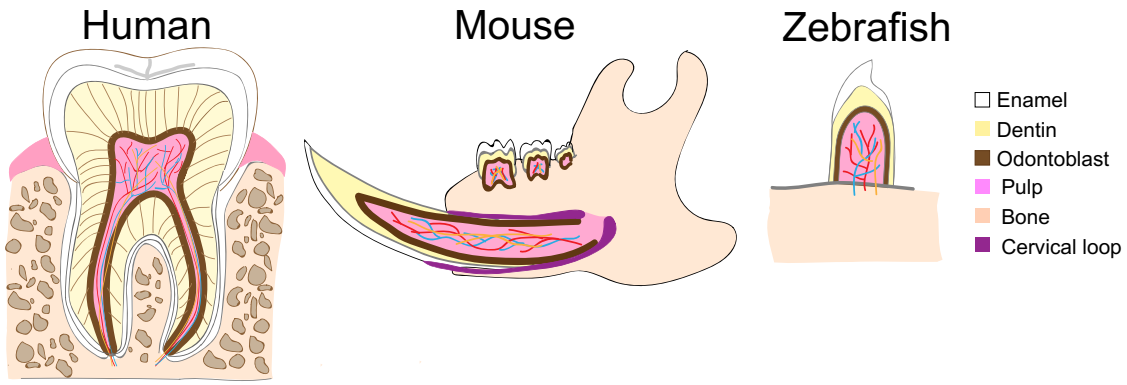

Fig. 5. Diagram illustrating analogous dental anatomy in human, mouse and zebrafish. Unlike human teeth, mouse have a continuously growing lower incisor from stem cells in the cervical loop. Zebrafish teeth are continuously replacing. However, zebrafish teeth do not have roots and the crown of the tooth is ankylosed to the bone.

This thesis study is based on the observation that *Rspo3* was identified as a target gene for *Irf6*. We focused on the role of *Rspo3* in regulating craniofacial pattern and differentiation. Using complementary zebrafish and mouse models, we detailed the gene expression of *Rspo3* during embryogenesis in craniofacial structures. We then interrogated the function of *Rspo3* by genetically targeting *Rspo3* in mouse and zebrafish. Through these studies, we uncovered an important role for *Rspo3* in modulating Wnt/β-catenin signaling in tooth development and bone homeostasis in the craniofacial complex.

HYPOTHESIS AND SPECIFIC AIMS

We hypothesize that *rspo3* function in the *irf6* regulatory pathway to regulate craniofacial development. Here, we focused on the role of *Rspo3* in regulating craniofacial patterning and differentiation, particularly in ossification and tooth formation.

Aim 1: to examine the effect of *irf6* mutant rescue on *rspo3* expression and the co-expression of *rspo3* and *irf6* during craniofacial development.

Aim 2: to describe the expression and function of *Rspo3* gene during embryonic development in zebrafish and mouse models.

Aim 3: to assess the role of *rspo3* in β-catenin mediated Wnt signaling in zebrafish.

Aim 4: to describe *rspo3* expression and function in dental and bone morphogenesis.

Significance

This research is based on our lab's previous discovery of *irf6* candidate genes with biological and clinical importance after integrating experimental, FaceBase and whole-genome sequencing (WGS) datasets. This study makes an important vertical gain of knowledge to link *Irf6* gene regulatory pathway to *Rspo3* modulator of Wnt signaling and the function of this gene in zebrafish and mouse models during craniofacial morphogenesis. Identification of modulators of Wnt signaling during development and homeostasis of adult skeletal tissues may lead to new insights into disease etiology and identify potential targets for therapeutic mediation.

Innovation

Our study aims provided novelty in addressing the gap in knowledge in *Rspo3* function in craniofacial development and palatal cleft pathogenesis and in its robust approaches which include the following:

- **Unique high resolution analysis of gene expression.**

  We utilized the novel RNAscope *in situ* hybridization technology to gain high resolution analysis of *Rspo3* gene expression in zebrafish and mice during craniofacial and dental development.

- **Rapid generation of loss-of-function mutants.**

  Zebrafish provided an excellent model for rapid functional analysis of *rspo3* candidate gene. We examined the genetic requirement of *rspo3* in zebrafish development, using complementary CRISPR/Cas9 mediated targeted mutagenesis and antisense morpholino (MO) oligomers to disrupt gene action.

- **Interaction between *Rspo3* and Wnt genes.**

  Our lab has developed several genetic models of Wnt pathway genes, including *wls*, *wnt5b* and *gpc4*. With these mutants in hand, we are able to interrogate genetic interactions with *rspo3*. Additionally, we acquired a *TCF/Lef:GFP* reporter line where dynamic canonical Wnt signaling can be visualized.

- **Performing cephalometric analysis in zebrafish skulls.**

  We developed new analytic tools to quantify craniofacial relationships in adult fish, using 3D cephalometric analysis obtained from micro-CT of zebrafish skulls to describe craniofacial malformation. One measurement to analyze the frontal bone bossing and the other measurement is to describe midface hypoplasia.

Experimental approaches

Aim 1: : to examine the effect of *irf6* mutant rescue on *rspo3* expression and the co-expression of *rspo3* and *irf6* during craniofacial development.

1.1- To determine the genetic and functional interaction between *irf6* and *rspo3* via zebrafish rescue assay.

1.2- To examine whether *irf6* and *rspo3 gene* expressions co-localize in the same cell by performing RNAscope *in situ* hybridization.

Aim 2: to describe the expression and function of *Rspo3* during embryonic development in zebrafish and mouse models.

2.1- Characterize *rspo3* expression via whole-mount RNA *in situ* hybridization (WISH).

2.2- Determine the type of cells expressing *rspo3* during craniofacial morphogenesis using RNAscope.

2.3- Describe *rspo3* function by morpholino mediated gene knockdown in zebrafish.

2.4- Perform CRISPR-Cas9 mediated gene targeting and characterize *rspo3* mutant zebrafish alleles.

Aim 3: to assess the role of *rspo3* in β-catenin mediated Wnt signaling in zebrafish.

3.1- Determine the effect of *rspo3* knockdown in TCF/Lef:GFP and sox10:mCherry transgenic reporter line.

3.2- To characterize the interaction between *rspo3* expression and Wnt-pathway genes (*wls*, *wnt9a* and *wnt5b*).

Aim 4: to describe *rspo3* expression and function in dental and bone morphogenesis.

4.1- Characterize *rspo3* expression in teeth by performing RNAscope *in situ* hybridiation.

4.2- Alizarin staining and micro-CT to identify significant difference in bone and dental development between *rspo3-/-* mutants and aged matched wild type zebrafish siblings.

4.3- Measure osteoclast activity in the craniofacial region via tartrate-resistant acid phosphatase (TRAP) in *rspo3-/-* mutant.

Materials and Methods

Experimental animals. All zebrafish (*Danio rerio*) experiments were approved by the Institutional Animal Care and Use Committee (IACUC), approval number: 2010N000106. Adult zebrafish and embryos were cared for and maintained in this study as described previously.[84] Mouse experiments were approved by IACUC, approval number: 2017N000050. Wild type mice were obtained from the Jackson Laboratory (C57BL/6J, Bar Harbor, ME, USA) and *Rspo3* mice were kindly provided to Dr. Baron by Dr. Christof Nierhs (German Cancer Research Center, Heidelberg, Germany). Tg(Wnt1-cre/ERT)1Alj/J mice were obtained from the Jackson Laboratory (008851).

Zebrafish CRISPR mutant line, morpholino knockdown and reporter lines.

We performed genome editing via CRISPR-Cas9 mutagenesis in zebrafish for functional analysis of *rspo3* mutant line targeting CCTGGCAGCCCTGGGAGCTC with -20 bp deletion (Fig. 14). The forward genotyping primer for *rspo3* line is 5'-AAGCAGCAAAAATAAGTTCCCA-3' and the reverse primer is 5'-CCACTCCCCATTGCTTTATTAC-3' with Fluoresce (FAM) modification on the reverse primer. Mutant peak is observed at 337bp and WT peak observed at 357bp.

In addition, we used translation blocking *rspo3* morpholino (MO) (5'-TGGAGATCAGTTGCAATTGCATAGT-3') and standard control oligo (5'-CCTCTTACCTCAGTTACAATTTATA -3') designed by Gene Tools, LLC (Philomath, OR, USA). Both MOs were diluted to 1.7 ng/nl and injected into one-cell stage zebrafish embryos using a microject 1000A microinjection system (Holliston, MA, USA). Transgenic lines Tg(*sox10*:mCherry)[10] and Tg (TCF/Lef-miniP:dGFP)[85] were also used in this study.

Whole-mount *in situ* hybridization.

Primers used to generate the *rspo3* RNA probe are forward primer 5'-AACCTGTGGCTTCAAATGG-3' and reverse primer 5'-TTGTTGTCGCTCATCCAGTA-3'[57]. *wls* probe is generated from forward primer 5'-ATTGCGGATGGAGCTTCGATC-3' and reverse primer 5'- ATAGATGCCAGTGAAGAAGGCA-3'. The forward primer for *wnt5b* probe production is 5'-AAGTGTCATGGCGTCTCAG-3' and reverse primer 5'-AAAAACCCTCTGTTGGAACC-3'. The forward primer for gpc4 probe generation is 5'-ACTGCTGGAGCGCATGTTTCGAC-3' and reverse primer 5'-CGATCCTTTCTCCAACACACACTG-3'. T7 promotor (gaaattaatacgactcactatagg) was added to all reverse primers. RNA products were checked by gel-electrophoresis and stored at -80°C until use. As described by Ling et al. [86], WISH in zebrafish was performed on wild type samples at 24 hpf and 48 hpf. Also, it was carried out in *rspo3*-MO (1.7 ng/nl) and standard oligos (1.7ng/nl) at 48 hpf.

Skeletal staining. Chondrocyte staining was performed using Alcian blue at 5 days post fertilization (dpf) for the MO experiment and 10 dpf for CRISPR mutant line as previously described.[87] The sample size (n) was 5 embryos per each group. The zebrafish ethmoid plate (corresponding to the mammalian palate) and lower jaw were dissected and mounted in 4% methyl cellulose prior to imaging. Whole-mount Alizarin staining was performed at 10 dpf in *rspo3* mutant and wild type zebrafish embryos (n= 5 wild type and 5 *rspo3*-/- mutants), as previously described.[88] Adult zebrafish bones and teeth were stained with Alizarin red according to previous study description.[89] Tartrate-resistant acid phosphatase (TRAP) protocol was adapted from previous study[90] and used as a histochemical marker for osteoclast activity.

Imaging was performed using Nikon Eclipse 80i microscope (Melville, NY, USA) and NIS-Elements Br imaging software version 4.40 (2015). Imaging was performed using Nikon Eclipse 80i microscope and NIS-Elements Br imaging software version 4.40 (2015).

RNAscope *in situ* hybridization and confocal imaging.

Sample preparation: 48 hpf and 5 dpf zebrafish embryos were fixed using 4% formaldehyde overnight at 4°C. The adult zebrafish (6 months old) and mouse (P7) dental structures with pharyngeal jaw were fixed using 4% formaldehyde overnight at 4°C then decalcified overnight using 0.35 M ethylenediaminetetracetic acid (EDTA) as previously described.[91] Mouse embryos at E13.5 were fixed with 4% formaldehyde overnight at 4°C. n= 3 zebrafish embryos and n=3 mouse embryos were analyzed.

In preparation for cryosectioning, all samples were placed in 15% sucrose (PBS) until the tissue sank followed by 30% sucrose (PBS) overnight at 4°C. Samples were cryo-embedded in OCT (Tissue-Tek, #4583) in coronal orientation. Sections (10 μ) were prepared using Leica CM1850 cryostat.

RNAscope probes: Dr-rspo3-C2 (catalog number: 555121-C2), Dr-col1a1-C2 (catalog number: 409491-C2), Dr-sox10-C3 (catalog number: 444698-C3), Dr-runx2a-C1 (catalog number: 409521), Mm-Rspo3-C3 (catalog number: 402011-C3), Mm-Col1a1-C2 (Catalog number: 319371-C2). All probes were manufactured by Advanced Cell Diagnostics (ACD; Newark, NJ, USA). Sample pre-treatment and RNAscope were performed according to the manufacturer's instructions (Advanced Cell Diagnostics, Newark, NJ, USA). Slides were imaged using Leica SP8 inverted confocal laser scanning microscope and the image processing was carried out using ImageJ version 2.0 (2018).

Immunohistochemistry and histological staining. Immediately following RNAscope *rspo3* gene detection in E13.5 coronal section, slides were washed with TBS twice for 2 min then blocked using 10% goat serum, 1% BSA, 0.1% TBST for 30 min at room temperature. Sections were treated with primary antibody (rabbit α-RUNX2, EPR14334, ab192256, Abcam, Cambridge, MA, USA) overnight at 4°C. The following day, as per ACD protocol (Newark, CA, USA) secondary antibody (goat α-rabbit Alexafluor 555, ab150078; Abcam, Cambridge, MA, USA) for 1 hr at room temperature.

Additionally, immunohistochemistry was performed using primary antibody (rabbit α-β catenin, ab16051, Abcam, Cambridge, MA, USA) and secondary antibody (goat α-rabbit Alexa fluor 555, ab150078, Abcam, Cambridge, MA, USA). Sections were imaged using Leica SP8 inverted confocal laser scanning microscope and the image processing was carried out using ImageJ version 2.0 (2018). n= 3 zebrafish embryos and n=3 mouse embryos were analyzed.

Micro-computed tomography. Wild type and *rspo3* mutant adult zebrafish were sacrificed at 6 month of age. The sample size (n) was 9 wild type and 7 mutant zebrafish. The fish were scanned as described by previously.[92] The voxel size of Micro-CT analysis was 10.5 μm. Images were reconstructed and viewed using Amira software version 6.

Measurement of bone mineral density. The reconstructed bitmap image (BMP) files were converted to NIfTI format for simplification, using Amira software. The threshold tool values were consistent between the samples (32-72 threshold logic unit). Each zebrafish skull was

segmented into bone elements (dentary, anguloarticular, premaxilla, maxilla and parasphenoid) using Amira manufacture's instruction. Hydroxyapatite calibration curves were prepared from images of hydroxyapatite phantoms, measured using ImagJ2 software (2015). High correlation (R^2=0.99973) was observed in the calibration curve. Bone mineral densities of the head and bone elements were measured, based on these calibrations. After that, bone volume of the head and bone elements were measured. n= 9 wild type and 7 mutant zebrafish were analyzed at 6 months of age.

Quantitative RT-PCR. Three independent samples of wild type and *rspo3* CRISPR/Cas9 mutant at 6 hpf were collected and measured in triplicate in order to characterize the *rspo3* mutant. We decided to collect embryos at 6 hpf, because it has been reported that *rspo3* mRNA is highly expressed in zebrafish embryos at this time point.[34] In addition, three independent samples of 1-cell stage wild type and 24 hpf wild type were collected and measured in triplicate in order to examine the presence of *rspo3* maternal transcript. RNA extraction was performed using RNeasy Mini Kit (Qiagen, Germantown, MD, USA). We used SuperScript First-Strand Synthesis System IV (Thermo Fisher Scientific, Grand Island, NY, USA) to synthesize first-strand cDNA. Quantitative reverse-transcription PCR (RT-PCR) was performed using *rspo3* Taqman probe (Dr03109282_m1, cat. #: 4351372) and normalized to 18s rRNA expression (Hs03003631_g1, cat. #: 4331182). Taqman™ fast advanced master mix (cat. #4444557, Thermo Fisher Scientific, Grand Island, NY, USA) and qPCR was performed using the StepOnePlus Real-Time PCR system (Applied Biosystems).

Statistical analysis. IBM SPSS statistics version 26 was used for all the statistical analysis. Student's t-test was used to compare between the two groups. Statistical significance was set at p-value ≤ 0.05. Asterisks in the figures indicate p-value ≤ 0.05. Data presented as means$\pm$ SEM.

Results

Genetic and functional interaction was found between *irf6* and *rspo3*.

The expression of *rspo3* was rescued by *irf6* mRNA injection into null *irf6* zebrafish embryos, which supports transcriptional activation of *rspo3* by *irf6.* Using qRT-PCR, the level of *rspo3* mRNA is decreased in *irf6* mutants compared to wild type *irf6.* After injecting wild type *irf6* mRNA into null *irf6* embryos, the *rspo3* level was rescued to wild type level suggesting functional interaction between *irf6* and *rspo3* (Fig. 6).

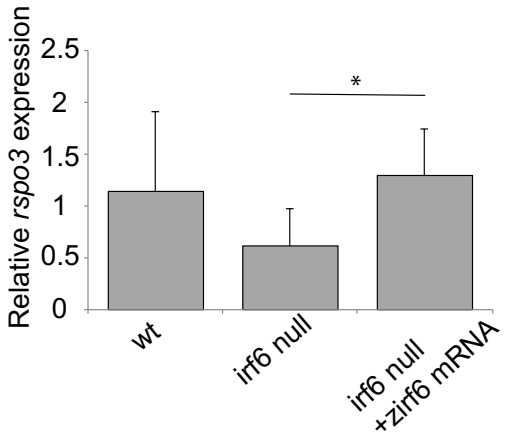

Fig. 6. qRT-PCR showing rescue of *rspo3* expression after *irf6* mRNA injection. *rspo3* expression is decreased in *irf6* mutant compared to wild type. After injecting *irf6* mRNA in *irf6* mutant, the *rspo3* expression is rescued indication genetic and functional interaction between *irf6* and *rspo3*.

Co-localization of *irf6* and *rspo3* expression in the pharyngeal arches and the palate during zebrafish embryonic development.

RNAscope *in situ* hybridization assay is more target-specific than traditional *in situ* hybridization with less background.[93] This analysis was carried out on wild type zebrafish embryos to test co-expression of *irf6* and *rspo3* (Fig. 7).

Zebrafish embryos at 24 hpf illustrated *rspo3* and *irf6* expression overlap at the telencephalon which is analogous to the cortical and subcortical brain regions in mammals (Fig. 7A).[94] In

addition, both genes overlap in zebrafish oral region at 24 hpf (Fig. 7B). Moreover, *rspo3* and *irf6* transcripts were found in the pharyngeal arches at 48 hpf (Fig. 7C, D). Interestingly, co-localization of *rspo3* and *irf6* expression were found in the palatal epithelium at 5 dpf in zebrafish (Fig. 7E). Similarly, we found *rspo3* and *irf6* transcripts in the first pharyngeal arch in mouse embryo at E13.5 (Fig. 7F).

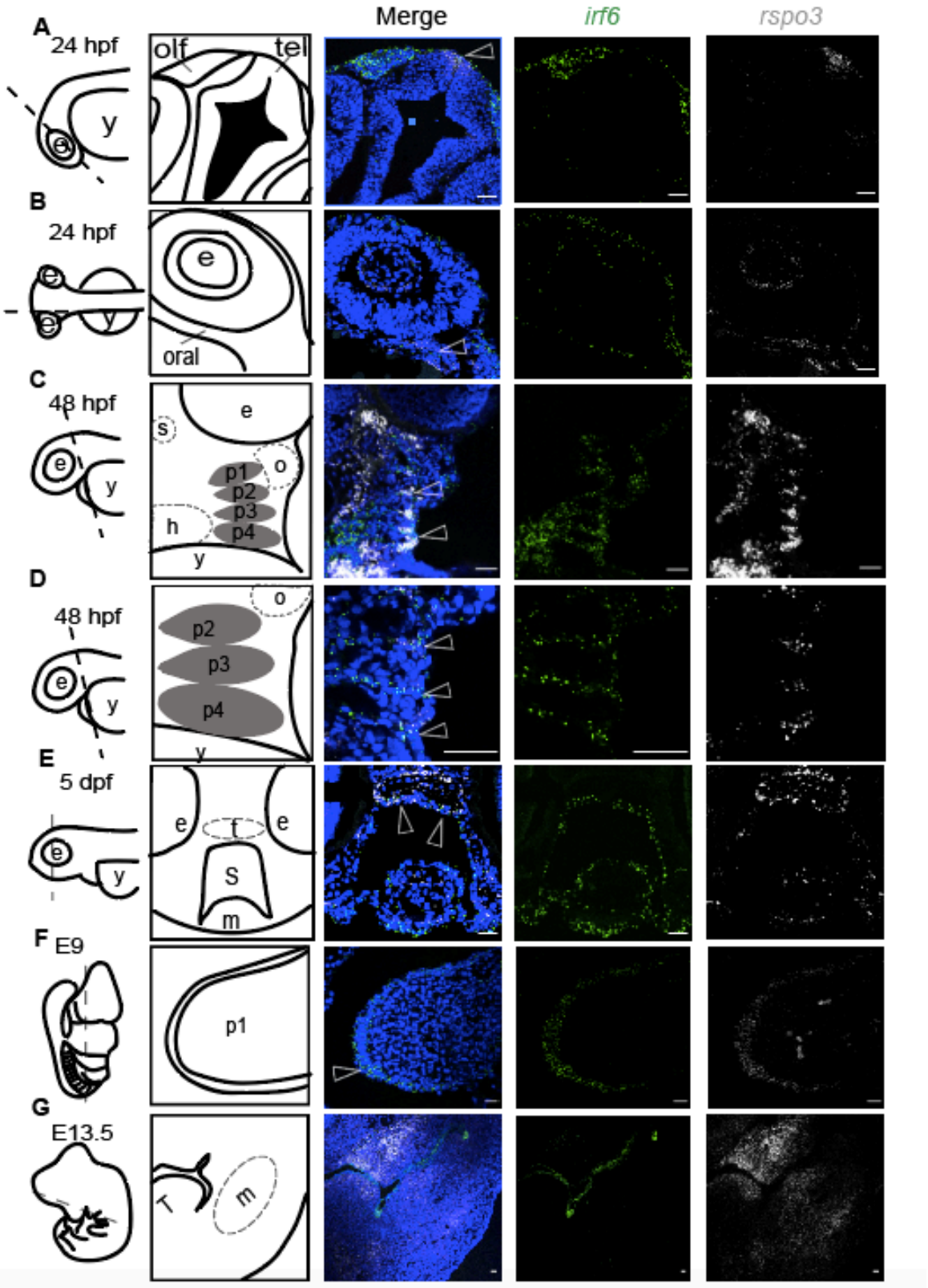
Merge
irf6
rspo3
A
24 hpf
olf
tel
y
e
B
24 hpf
e
oral
C
48 hpf
s
o
p1
p2
p3
p4
h
D
48 hpf
E
5 dpf
t
S
m
F
E9
G
E13.5
T
m

Fig. 7. Co-localization of *irf6* and *rspo3* expression in the pharyngeal arches and the palate during zebrafish and mouse embryonic development. Lateral views of zebrafish embryo demonstrating the level of each section, at 24 hpf, 48 hpf, and 5 dpf. In addition, lateral views of mouse embryo at E13.5 showing the level of section. A) *rspo3* is co-expressed with *irf6* in the telencephalon (open arrow). B) Zebrafish oral cells are double positive for *rspo3* and *irf6* transcripts at 24 hpf (open arrow). C) *rspo3* is marking the segmented paired pharyngeal pouches in cells and co-expressed with *irf6* transcripts (open arrow). D) At a higher magnification, co-localization of *rspo3* and *irf6* transcripts are identified in the pharyngeal pouch mesenchyme (open arrow). E) a more anterior coronal section shows *rspo3* transcripts are detected in the palate, and some palatal cells are double positive for *rspo3* and *irf6* (open arrow). F) Co-expression of *Rspo3* and *Irf6* in the first pharyngeal arch at E 9. G) At E13.5, we observed no co-expression of *irf6* and *rspo3* in the coronal section. Abbreviations: e: eye, h: heart, m: Meckel's cartilage, o: otic capsule, olf: olfactory placode, p1-p4: pharyngeal pouches, s: stomodeum, t: trabecula, tel: telencephalon, y: yolk sac. Scale bar: 25 μm

Expression of *Rspo3* in craniofacial region and in the perichondrial and osteoprogenitor cells during craniofacial morphogenesis.

Gene expression pattern of *rspo3* during embryogenesis was delineated by whole-mount RNA *in situ* hybridization (WISH). *rspo3* expression was detected in the brain, otic placode, endodermal pouches, ethmoid plate (hereafter palate) and Meckel's cartilage at 24 and 48 hpf (Fig. 8).

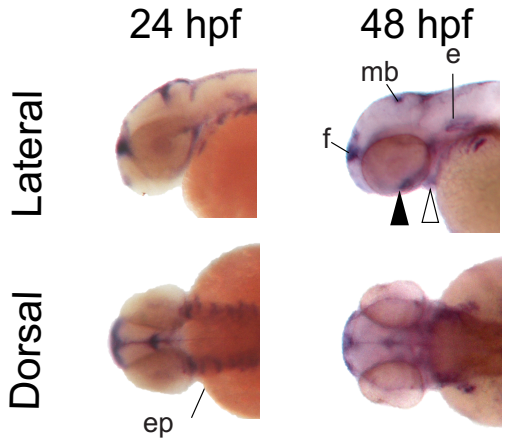

Fig. 8. Whole-mount RNA in situ hybridization demonstrating *rspo3* gene expression. *rspo3* transcripts were found in the forebrain (f), midbrain (mb) otic placode (o), endodermal pouches (ep), ethmoid plate (hereafter palate) (solid arrow) and Meckel's cartilage (open arrow) at 24 and 48 hpf in lateral and dorsal views.

Using RNAscope, we identified *rspo3* transcripts in perichondrial cells that circumscribe the *sox10* marked chondrocytes in the paired maxillary derived trabeculae and in Meckel's cartilage at 48 hpf and 5 dpf (Fig. 9A,D,E). In addition, *rspo3* gene expression was detected in the pharyngeal pouches at 48 hpf (Fig. 9B,C).

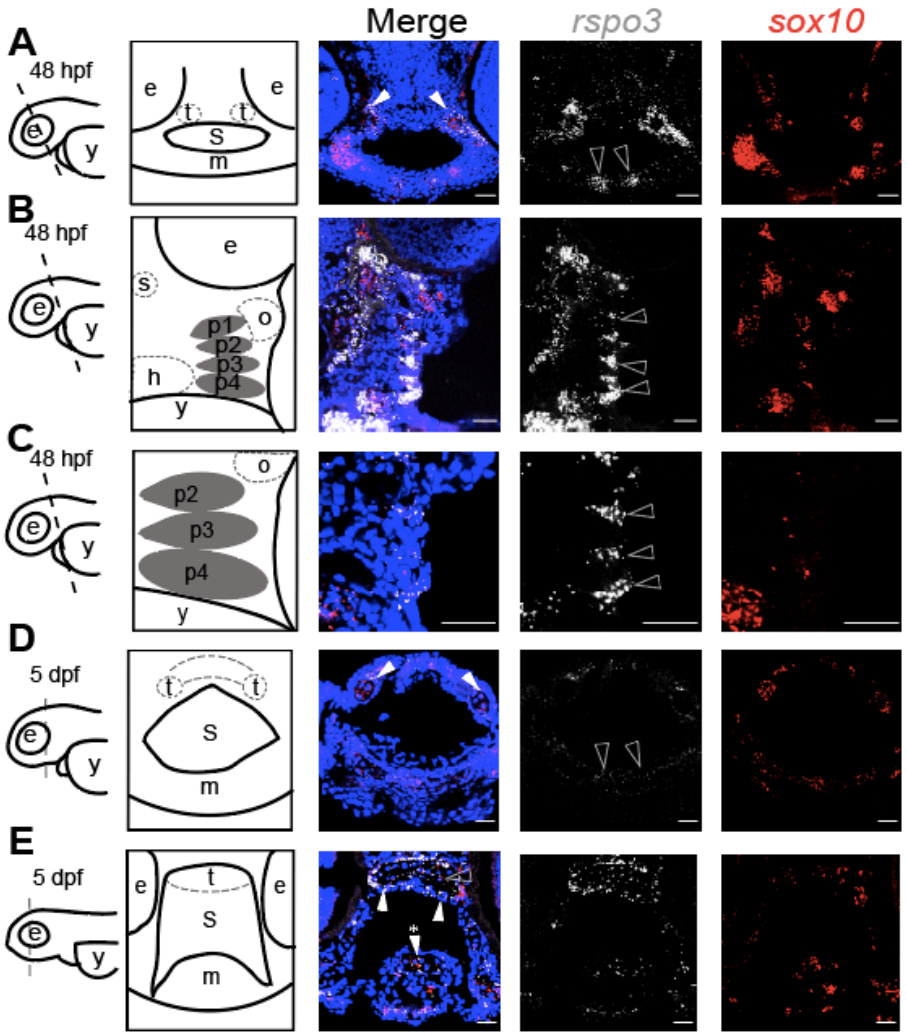

Fig. 9. *rspo3* transcripts were detected in the perichondrium, pharyngeal arches, palate and Meckel's cartilage in zebrafish. Lateral views of zebrafish embryo demonstrating the level of each coronal section, at 48 hpf, and 5 dpf. A) At 48 hpf *rspo3* transcripts are localized in cells that circumscribe the *sox10* marked chondrocytes in the palate trabeculae (solid arrow) and in Meckel's cartilage (open arrow). B) *rspo3* is marking the segmented paired pharyngeal pouches in cells (open arrows) that are juxtaposed to the *sox10* positive chondrocytes. C) At a higher magnification, *rspo3* transcripts are identified in the pharyngeal pouch mesenchyme (open arrow). D) At 5 dpf, *rspo3* transcripts continue to be expressed by cells the surround *sox10* marked chondrocytes in the palate trabeculae (solid arrow) and circumscribe chondrocytes of Meckel's

cartilage (arrow). E) A more anterior coronal section shows *rspo3* transcripts are detected in cells around (solid arrow) *sox10* positive cells in the palate, and some chondrocytes are double positive for *rspo3* and *sox10* (open arrow) in the palate and Meckel's cartilage (solid arrow with asterisk). Abbreviations: e: eye, h: heart, m: Meckel's cartilage, o: otic capsule, p1-p4: pharyngeal pouches, s: stomodeum, t: trabecula, y: yolk sac. Scale bar: 25 μm

To define the cell type expressing *rspo3* during skeletal development, we examined the localization of *col1a1* (perichondrium marker) and *rspo3* around the trabeculae of zebrafish embryos at 48 hpf (Fig. 10A,B). At 5 dpf, co-localization of *col1a1* and *rspo3* was observed around the palatal cartilage. However, *rspo3* is also expressed in the palate cartilage and has a broader and more diffuse gene expression (Fig. 10A,B). To determine whether gene expression in zebrafish correlates with mouse expression, coronal sections of E13.5 mouse embryos were examined for expression of *Rspo3* and *Col1a1* by RNAscope. In the mouse embryo, *Rspo3* transcript was similarly detected in the perichondrium of Meckel's cartilage, but *Rspo3* was also detected in Meckel's chondrocytes (Fig. 10C,D). We also investigated whether osteoprogenitor cells express *rspo3* by examining the expression of *runx2*, which is expressed in neural crest derived osteoprogenitor cells.[95-97] RNAscope analysis revealed co-expression of *runx2a* and *rspo3* around the trabeculae of zebrafish embryo at 48 hpf and at 5 dpf (Fig. 10B), however not all *runx2* positive cells expressed *rspo3*. This was similar to the expression of *Rspo3* and *Runx2* in E13.5 mouse embryos (Fig. 10C,D). These data demonstrate that *Rspo3* is expressed broadly, in perichondrial cells around palate and Meckel's cartilage, including osteoprogenitor cells that are *Runx2* positive.

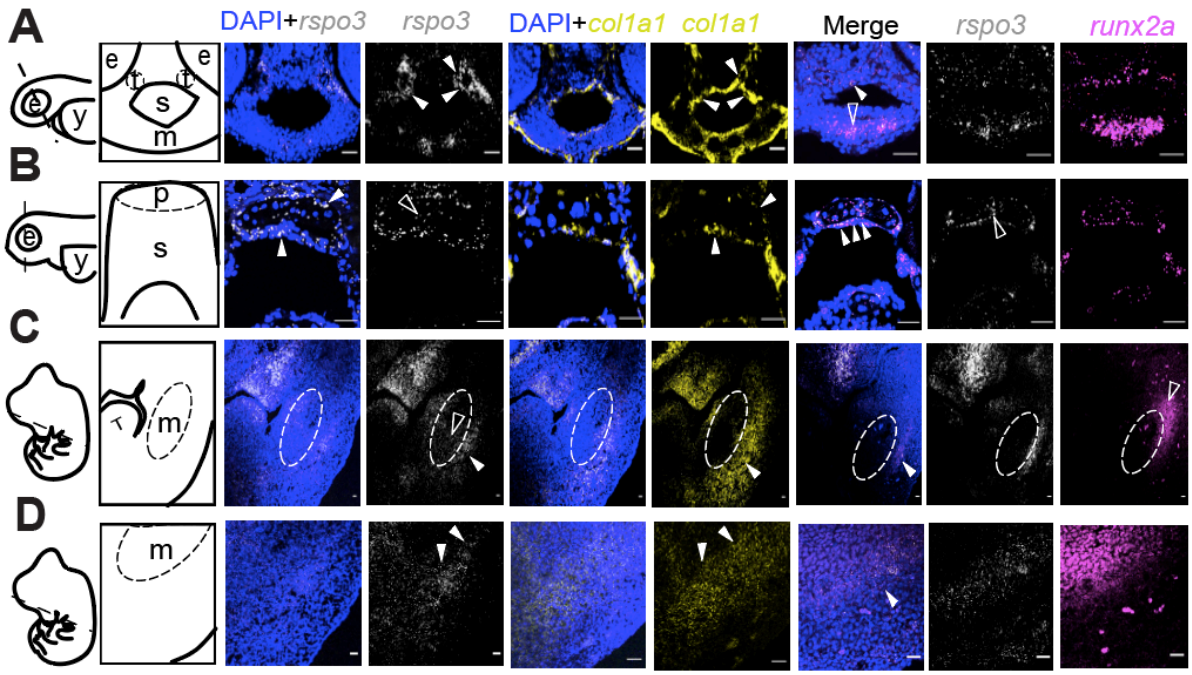

Fig. 10. Perichondrium and osteoprognitor cells express *Rspo3* during zebrafish and mouse development. A) RNAscope showing co-expression of *col1a1* and *rspo3* (solid arrow) around the trabeculae of zebrafish palate. In addition, co-expression of *rspo3* and *runx2a* in the palate (solid arrow) and Meckel's cartilage (open arrow) in coronal section of zebrafish embryo at 48 hpf. B) At 5 dpf, the coronal section demonstrates co-localization of *rspo3*, *col1a1* and *runx2a* transcripts around the palatal cartilage (solid arrow). However, *rspo3* is also expressed in some of the palate chondrocytes and has more diffuse expression (open arrow). C) Coronal section of E13.5 mouse embryo revealed co-expression of *Rspo3* and *Col1a1* in the perichondrium of Meckel's cartilage (solid arrow), but *Rspo3* transcripts are also detected in Meckel's cartilage cells (open arrow). In addition, co-localization of *Rspo3* and *Runx2* (solid arrow), but *Runx2* transcripts expression is more diffuse (open arrow). D) At a higher magnification, *Rspo3* and *Col1a1* are co-localized in the perichondrium of Meckel's cartilage. Also, *Rspo3* and *Runx2* are co-expressed. Abbreviations: d: dental, m: Meckel's cartilage, p: palate, t: tongue. Scale bar: 25 μm

Rspo3 is expressed in the mandibular condyle of mice.

Previous studies reported that patients with osteogenesis imperfecta have mutations in *COL1A1* which is expressed in the mandibular condyle and characterized by frontal bossing, midface hypoplasia and dentinogenesis imperfecta.[98,99] Since our data showed co-expression of *Rspo3* and *Col1a1* in the perichondrium of Meckel's cartilage and periosteum of the mandibular bone during embryogenesis in mice and zebrafish, these two genes could be functionally associated. Therefore, we investigated *Rspo3* expression in the mandibular

condyle. We found co-expression of *Rspo3* and *Col1a1* in the mandibular condyle in mice at postnatal day 7 (P7) (Fig. 11). A summary of cells expressing *Rspo3* with epithelial, chondrocyte, perichondrium and osteoprogenitor markers is shown in Fig. 12.

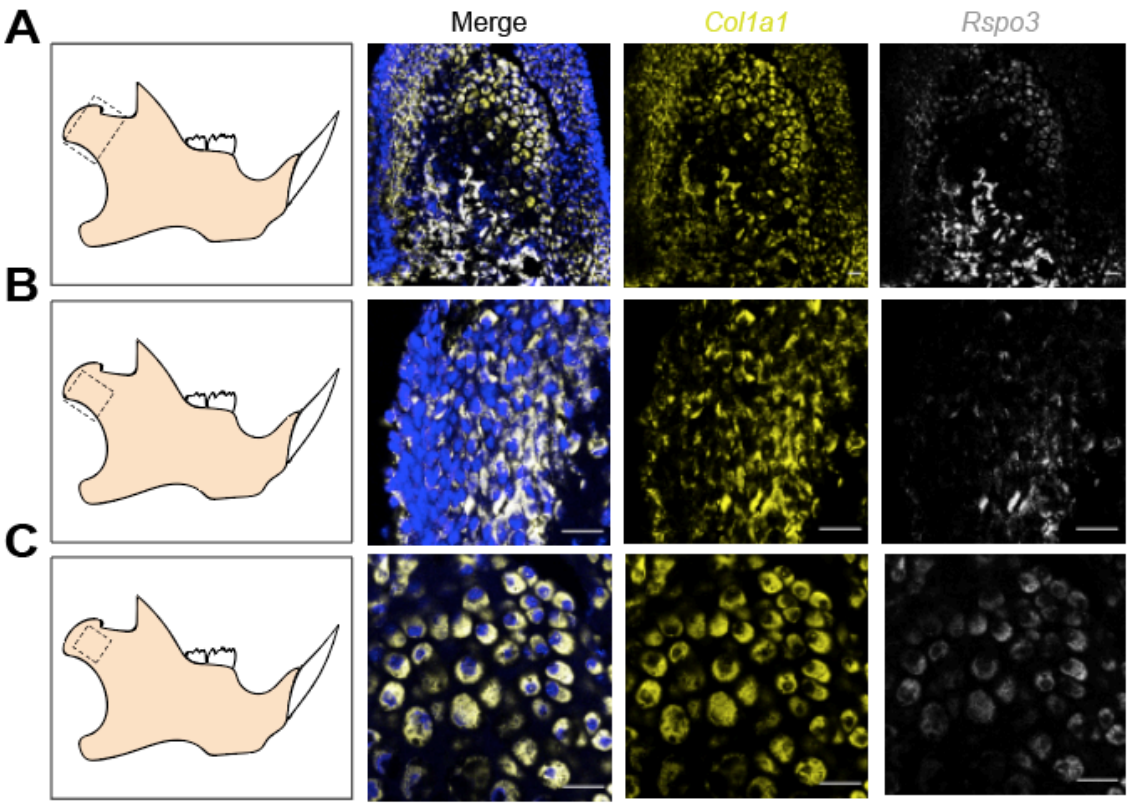

Fig. 11. *Rspo3* is co-expressed with *Col1a1* in mouse mandibular condyle. A) *col1a1* is co-expressed with *Rspo3* in the mandibular condyle. B) higher magnification showing double expression of *Col1a1* and *Rspo3* in the deeper layers of the condyle. C) Higher magnification demonstrating chondrocyte expressing both *Col1a1* and *Rspo3* in the condyle.

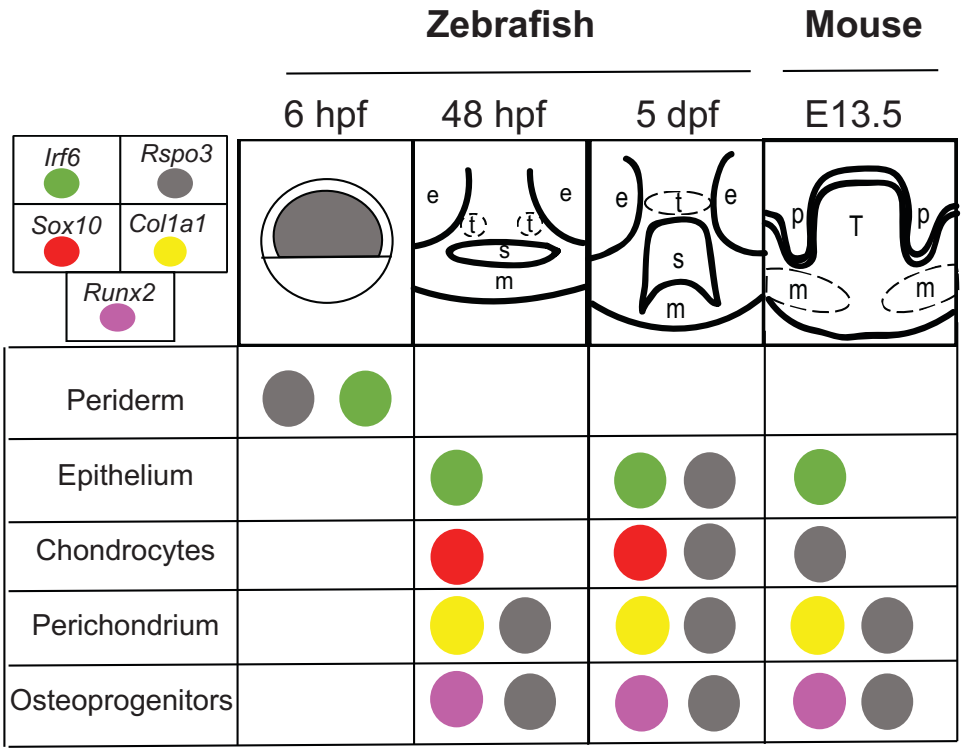

Fig. 12. Diagram summarizing the cells expressing *Rspo3* during zebrafish and mouse embryogenesis. In zebrafish, *rspo3* is co-expressed with *irf6* in periderm and epithelium at 5 dpf. Moreover, chondrocytes are expressing both *rspo3* and *sox10* at 5 dpf. In both zebrafish and mouse, perichondrium and osteoprogenitor cells are expressing *rspo3* during development. e: eye, m: Meckel's cartilage, p: palate, s: stomodeum, t: tongue.

rspo3 knockdown during embryogenesis and *rspo3* knockout results in palate and Meckel's cartilage dysmorphogenesis and osteogenesis defect.

Given the specific expression of *rspo3* in the palate and Meckel's cartilage regions, we interrogated *rspo3* function using anti-sense morpholino oligomer (MO) mediated protein depletion. Dose titration was carried out and determined that 1.7 ng/nl is the lowest dose that provided the most consistent phenotype without obvious toxicity in zebrafish embryos. Fig. 13B tabulates the percentage count of normal (blue), mild phenotype (orange), severe phenotype (gray) and dead embryos (yellow) after injecting standard oligo (1.7 ng/nl) and *rspo3-MO* (1.7 ng/nl) in embryos. At 5 dpf, we observed mild phenotype characterized with

cardiac edema, cleft palate, and malformation in the Meckel's cartilage, and a more severe phenotype showing cardiac edema, small cranium, missing palate and distorted Meckel's cartilage (Fig. 13A). The fish with mild and severe phenotype did not survive beyond 8 dpf.

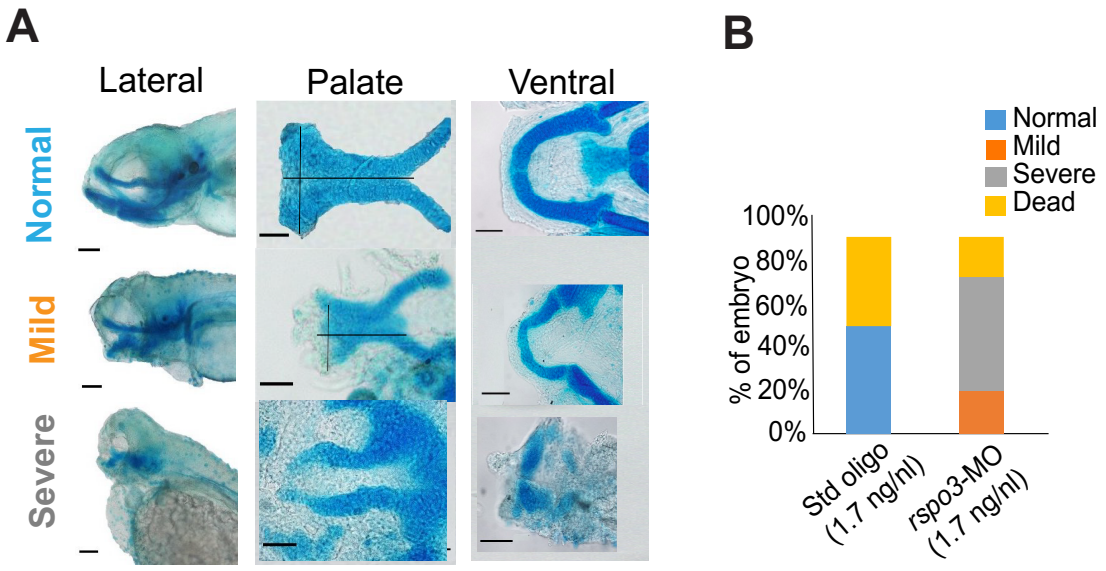

Fig. 13. Functional analysis of *rspo3* knockdown in zebrafish. A) Lateral views of Alcian blue stained embryos at 5 dpf showing the normal, mild phenotype and sever phenotype. In addition, there is a significant disruption of palate and Meckel's cartilage morphology in the *rspo3*-MO injected phenotypes compared to standard oligo injected embryos (control). B) Bar chart demonstrating the percentage of normal (blue), mild phenotype (orange), severe phenotype (gray) and dead embryos (yellow) after injecting standard oligo mopholino (1.7 ng/nl) and *rspo3*-MO (1.7 ng/nl), assaying phenotype of embryonic craniofacial cartilages by Alcian blue staining as show in A.

To further assess the genetic requirement of *rspo3*, we used CRISPR/Cas9-mediated genome editing to generate *rspo3* mutant alleles. Guide RNA targeting *rspo3* gene in Exon2 was used to generate and breed the mutant line (Fig. 14). A frameshift mutation was generated by a -20 base pair deletion, detected by microsatellite genotyping and confirmed by Sanger sequencing. This *rspo3* -20bp deletion allele (hereafter called *rspo3*-/-) was characterized by qRT-PCR at 6 hpf, where we observed that *rspo3* mRNA was significantly reduced in the mutant compared

to wild type (p-value<0.05). We decided to collect embryos at 6 hpf, because it has been reported that *rspo3* mRNA is highly expressed in zebrafish embryos at this time point.[34]

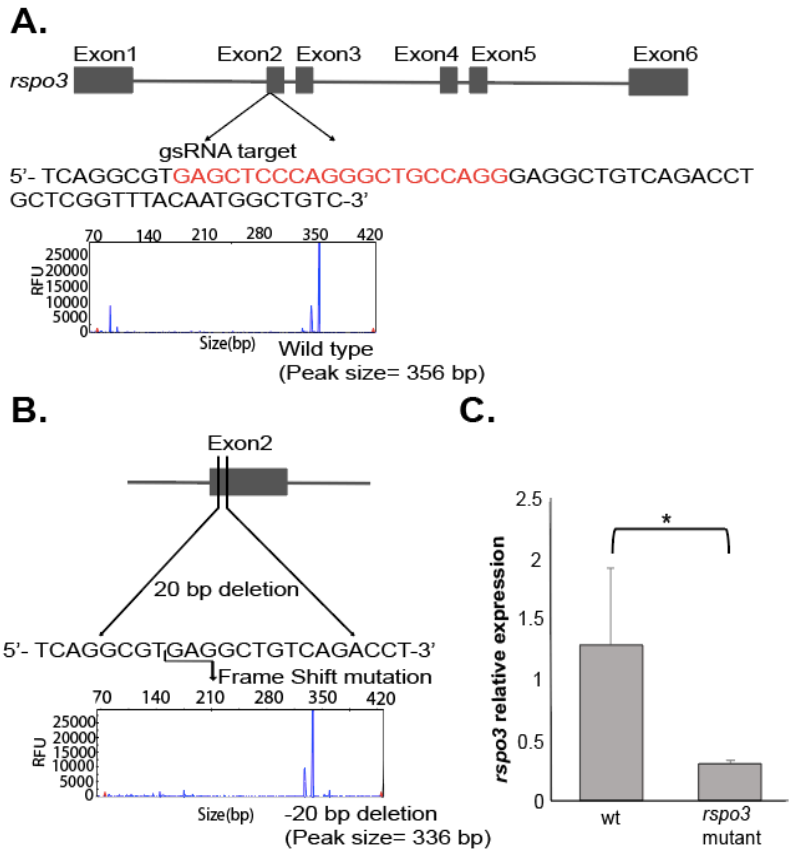

Fig. 14. Generation and characterization of CRISPR-Cas9 targeted *rspo3* allele in zebrafish. A) Guided RNA target is designed in *rspo3* Exon2 at the indicated sequence (red) for CRISPR-Cas9 mediated gene editing. Microsatellite genotyping presenting the wild type allele with peak size=356 bp. B) Frame shift mutation is generated with -20 base pairs micro-deletion. Microsatellite genotyping presenting the mutant allele with peak size=336 bp. C) Characterization of *rspo3*-/- and wild type by qRT-PCR at 6 hpf. The mRNA levels are significantly reduced in *rspo3*-/- compared to age matched wild type, likely consequence of mRNA nonsense mediated decay *($p \leq 0.05$). RFU: Relative fluorescence units.

To characterize the requirement of *rspo3* during embryonic craniofacial morphogenesis, Alcian blue staining was performed at 10 dpf, which showed consistent differences between wild type and *rspo3*-/- mutant embryos. Lateral views of wild type and *rspo3*-/- mutant zebrafish embryos are illustrated in Fig. 15A. The ceratohyal cartilage was slightly malformed in *rspo3*-/- mutants as compared to age matched wild type siblings (Fig. 15A). This difference

between gene knockdown and CRISPR knockout can be due to morpholino off-target effects or gene compensation by other *rspo* family members such as *rspo2* in the CRISPR-Cas germline *rspo3* -20bp deletion allele. Therefore, to test for this, *rspo2*-MO was injected into *rspo3*-/- single cell stage embryos, resulting in additional phenotypes including disrupted palate and Meckel's cartilage morphology and cardiac edema, conditions that were masked by *rspo2* gene compensation in *rspo3*-/- mutants (Fig. 15C,D). Knockdown *upf1* was reported to reduce mRNA decay and reduce effects of genetic adaptation.[100] We found similar phenotypes in *rspo3*-MO embryos, and in *upf1* MO injected *rspo3* -/- mutants (Fig. 15C,D), indicating that transcriptional adaptation was likely not occurring in *rspo3*-MO embryos.

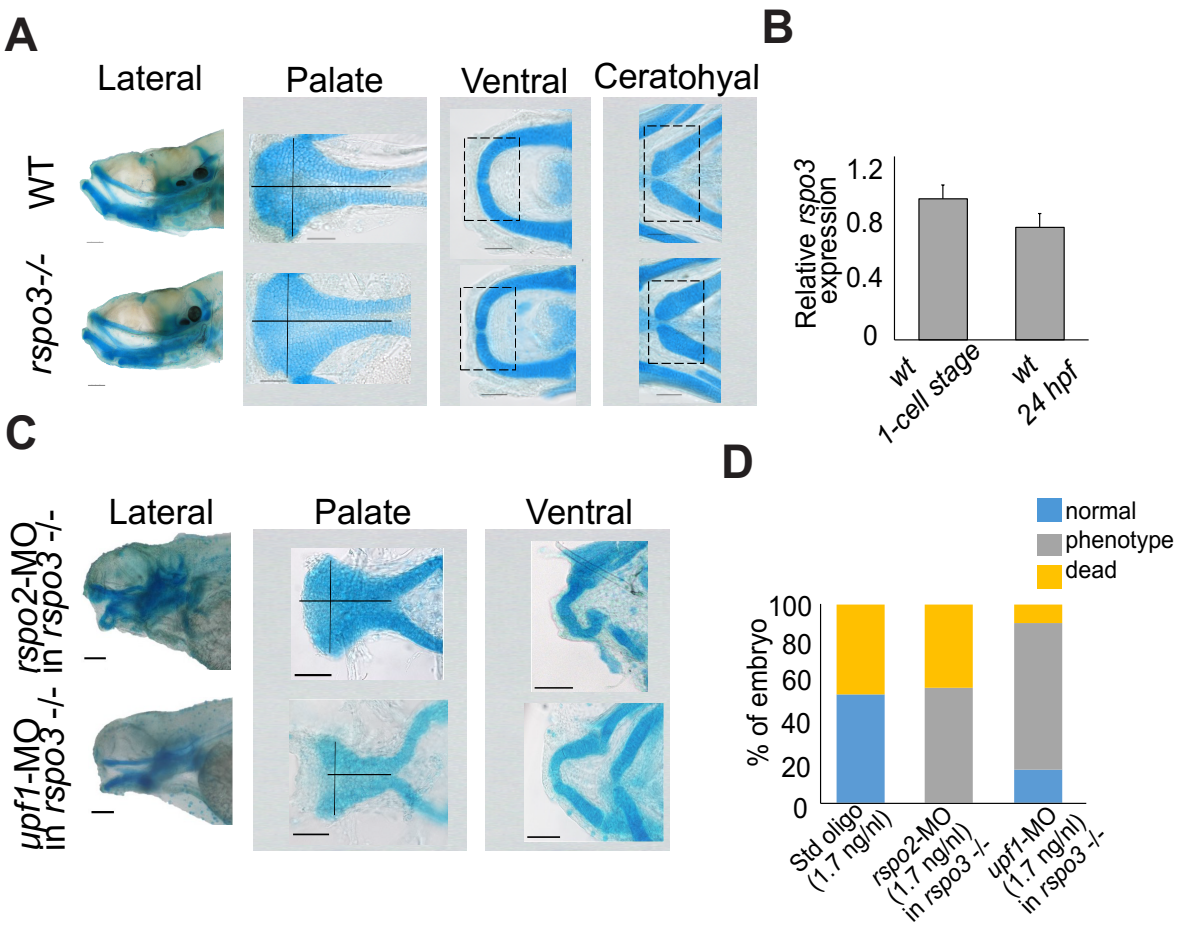

Fig. 15. Mutant allele of *rspo3* was generated using CRISPR mediated mutagenesis. *rspo3-/-* mutant females were generated to eliminated maternal contribution to embryogenesis. Mating of *rspo3-/-* females to *rspo3+/-* males produced 50% *rspo3+/-* embryos, and 50% *rspo3-/-* progeny, all without maternal *rspo3* mRNA. A) Lateral views of 10 dpf Alcian blue stained wild type and *rspo3-/-* embryos. The palatal cartilage looked similar in mutant and wild-type samples. The anterior of Meckel's cartilage is mildly malformed in *rspo3* mutant compared to age matched wild type siblings. B) qRT-PCR showing maternal transcript of *rspo3* in wild type at one-cell stage. C) Lateral view of Alcian blue stained embryos at 5 dpf after injecting *rspo2*-MO and *upf1*-MO in *rspo3*-/- embryos. We found a significant disruption of palate and Meckel's cartilage morphology and cardiac edema in the *rspo2*-MO and *upf1*-MO injected in *rspo3* -/- compared to standard oligo injected embryos (controls). Therefore, the phenotype presented after injecting *rspo2*-MO and *upf1*-MO in *rspo3* -/- looked similar to *rspo3*-MO phenotype suggesting that *rspo2* compensation could be masking the *rspo3*-/- phenotype. D) Bar chart demonstrating the percentage of normal (blue), phenotype (gray) and dead embryos (yellow) after injecting standard oligo mopholino (1.7 ng/nl), *rspo2*-MO (1.7 ng/nl) and *upf1*-MO (1.7 ng/nl). We found increased percentage of phenotype in *rspo3*-/- injected with *rspo2*-MO and *upf1*-MO indicating gene compensation masking the phenotype in *rspo3*-/-. The phenotype of embryonic craniofacial cartilages is assayed by Alcian blue staining as show in C. WT: wild type, Scale bar: 10 μm.

Rspo3 global deletion in the mouse is embryonic lethal.

At E11, the *Rspo3-/-* embryo is under-developed due to developmental arrest prior to E10.5 (Fig. 16).

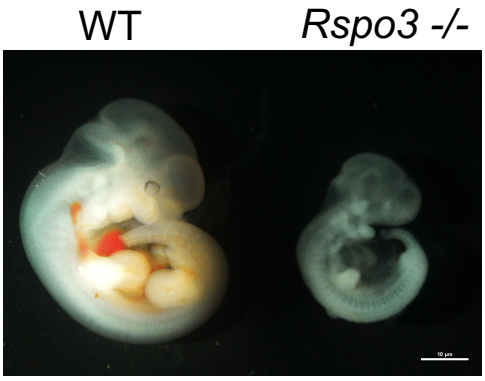

Fig. 16. *Rspo3* global deletion in the mouse is embryonic lethal. At E11, mouse embryo with *Rspo3* mutation is under-developed due to developmental arrest prior to E10.5. Scale bar: 10 μm

No phenotype was found in *Wnt1*-cre/+; *Rspo3* $^{flox/flox}$ mice.

In order to investigate the role of *Rspo3* in neural crest cells, *Rspo3* was specifically ablated in *Wnt1*-expressing cells. We created in *Wnt1-Cre*/+; *Rspo3* $^{flox/flox}$ mice. As a control we

used *Wnt1-Cre*/-; *Rspo3* $^{wt/wt}$. No significant differences were found in craniofacial bone and teeth in *Wnt1-Cre*/+; *Rspo3* $^{flox/flox}$ mice compared to *Wnt1-Cre*/-; *Rspo3* $^{wt/wt}$ (Fig. 17).

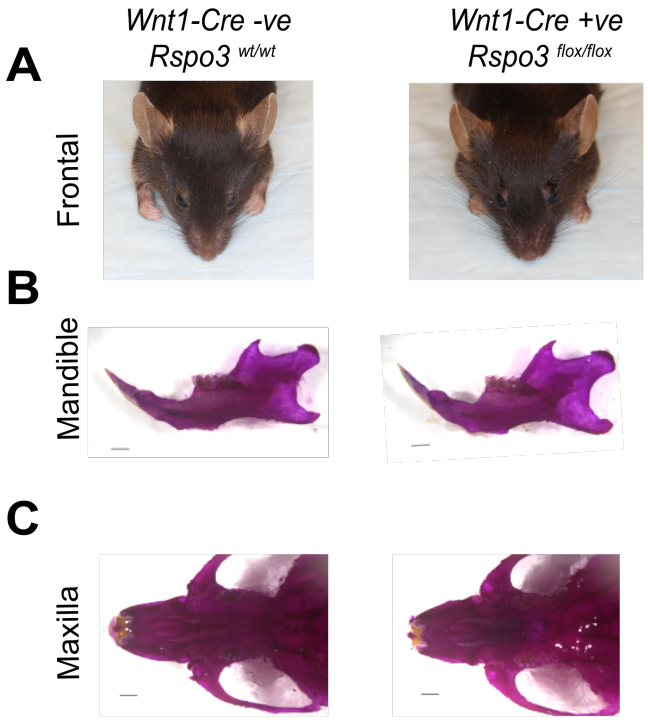

Fig. 17. No differences were found between *Wnt1-Cre*/+; *Rspo3* $^{flox/flox}$ and *Wnt1-Cre*/-; *Rspo3* $^{wt/wt}$. A) Frontal photos of *Wnt1-Cre*/+; *Rspo3* $^{flox/flox}$ and *Wnt1-Cre*/-; *Rspo3* $^{wt/wt}$ showing minor differences. B) Lateral views of alizarin stained lower jaw showing no significant differences. C) Alizarin stained skull demonstrating no differences between *Wnt1-Cre*/-; *Rspo3* $^{wt/wt}$ and *Wnt1*-cre/+; *Rspo3* $^{flox/flox.}$ wt: wild type

Canonical β-catenin mediated Wnt signaling activity is suppressed by disruption of *rspo3*.

To assess the role of *rspo3* in β-catenin mediated Wnt signaling, *rspo3*-MO was injected into single cell stage TCF/Lef:GFP and sox10:mCherry transgenic reporter line zebrafish embryos.[85] Knockdown of *rspo3* caused reduction of TCF/Lef:GFP expression (Fig. 18A). We also tested expression of wnt genes (*wls, wnt5b, gpc4*) in *rspo3*-MO morphants using WISH. Our results show reduced *wnt5b* expression in *rspo3*-MO compared to standard oligo injected embryos (1.7ng/nl) (Fig. 18B). On the other hand, *wls* and *gpc4* expression was increased and

more diffuse in *rspo3*-MO in relation to control (Fig. 18B). These results indicated that *rspo3* affect Wnt/β-catenin activity during zebrafish craniofacial morphogenesis.

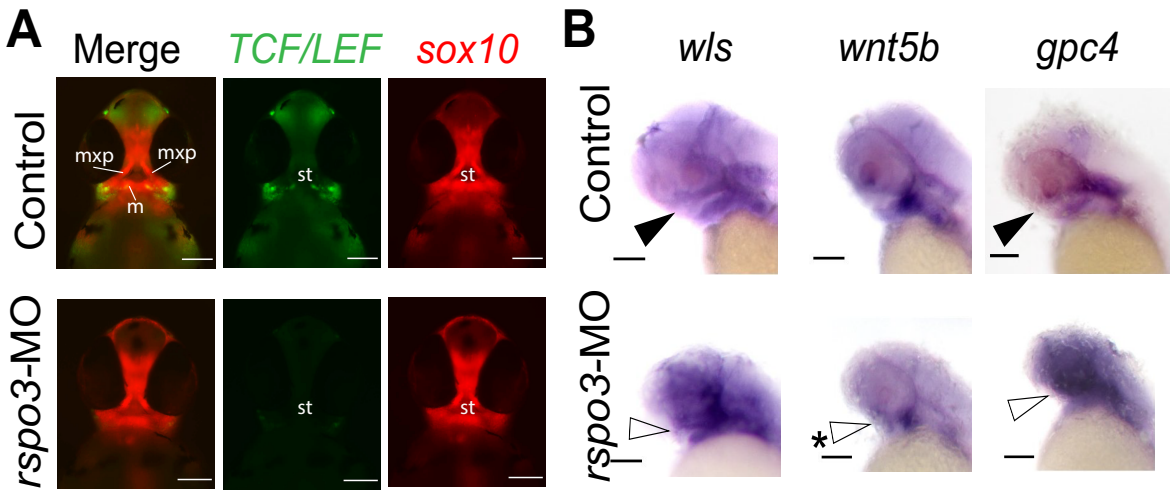

Fig. 18. Disruption of *rspo3* affect β-catenin mediated Wnt signaling. The *TCF/Lef:GFP* transgenic reporter line was previously described to label the craniofacial domain, useful to assess wnt signaling status during craniofacial morphogenesis. At 48 hpf, the *TCF/Lef:GFP* signal is highly expressed in the oral pharyngeal epithelium and is visible around the stomodeum (st). Injection of control standard MO oligo and *rspo3*-MO was carried out and the transgenic lines were imaged to 48 hpf, when craniofacial morphogenesis is taking place during embryogenesis. A) Coronal section of 48 hpf zebrafish showing reduced *TCF/Lef:GFP* expression in *rspo3*-MO injected embryos. In the control embryos, *sox10:mCherry* labeled neural crest derived chondrocytes label the cartilage structures such as maxillary prominences (mxp) converging to form the palate, and the merging mandribular prominences that form Meckel's cartilage (m). The control was standard oligo (1.7ng/nl). B) Whole-mount RNA in situ hybridization demonstrating *wls, wnt5b and gpc4* genes expression in *rspo3*-MO (1.7 ng/nl) at 48 hpf. *wls* and *gpc4* gene expression is increased in *rspo3*-MO (open arrow) compared to control (solid arrow). However, *wnt5b* is reduced in *rspo3*-MO (open arrow with asterisk) compared to wild type. The control is standard oligo (1.7ng/nl). Scale bar: 25 μm.

rspo3 is expressed in dental progenitor cells.

In addition to examining *Rspo3* requirement in osteogenesis and morphogenesis of craniofacial bones, we also investigated *Rspo3* requirement in tooth formation. We observed co-localization of *rspo3* and *col1a1* (odontoblast marker) transcripts in odontoblasts and the crypt epithelium that surround the tooth in zebrafish. Further, *rspo3* is more broadly and diffusely expressed in the dental pulp of the tooth structure in zebrafish (Fig. 19A,B,C). Interestingly,

whereas *col1a1* is expressed in all zebrafish teeth, the expression of *rspo3* was restricted to replacement teeth, characterized by coalesced odontoblast progenitor cells present in the center of the tooth pulp, and not in differentiated odontoblasts lining the inner dentin surface (Fig. 19A). Furthermore, β-catenin is active in odontoblasts, surrounding the pulp and crypt epithelium in zebrafish β-catenin immunohistochemistry (Fig. 19D).

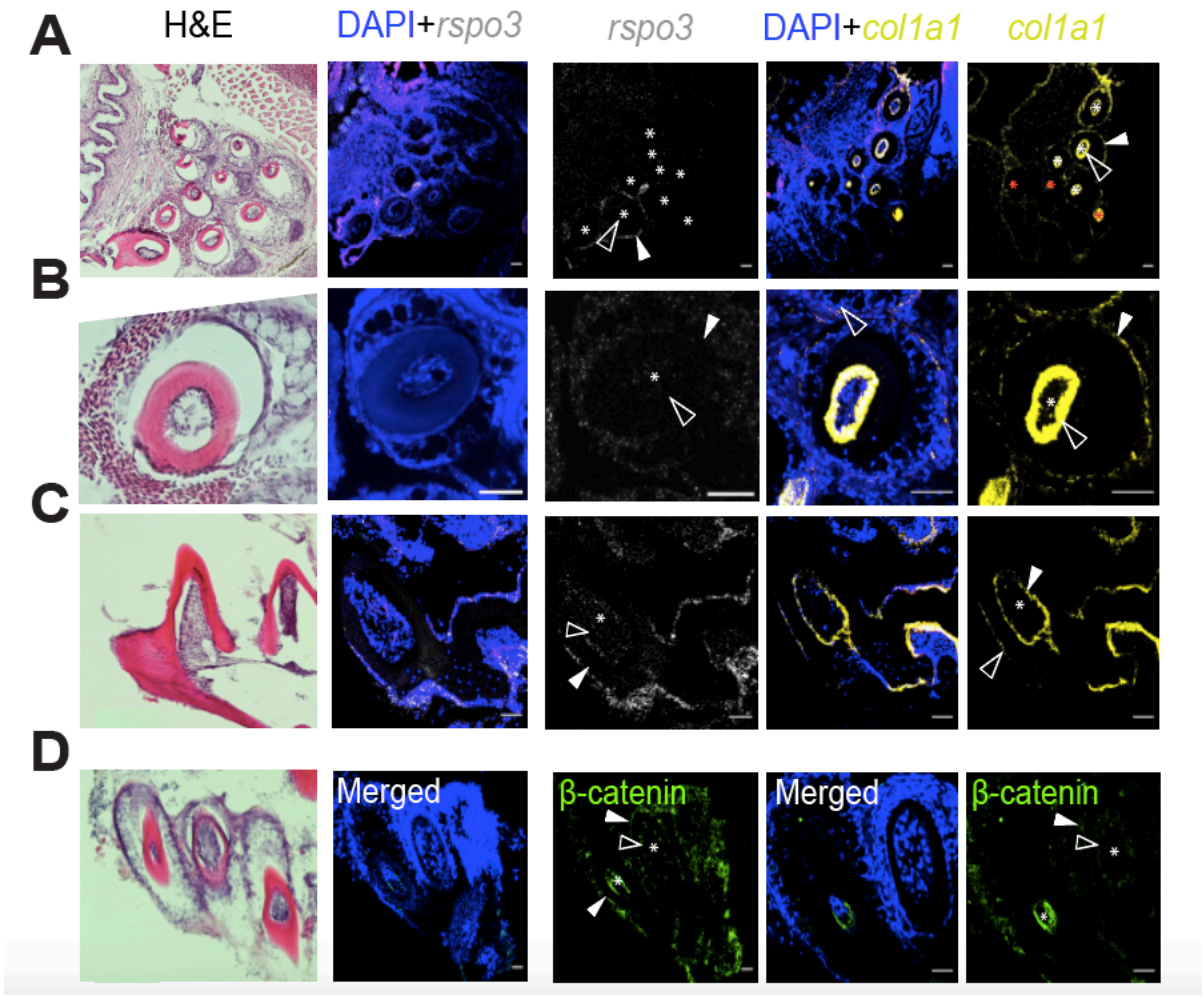

Fig. 19. *rspo3* expression in zebrafish dental structure. RNAscope gene expression analysis of *rspo3* and *col1a1* in coronal and sagittal sections of adult zebrafish (180 dpf), focusing on dental structures. The H&E staining in A,B,C and D are different sections than the RNAscope sections. A) *rspo3* is more diffusely expressed in the epithelial crypt (solid arrow) and in the odontoblasts (open arrow), but labels some but not all the teeth (asterisks placed over each tooth pulp). In contrast, and *col1a1* transcripts are detected at high levels in odontoblasts (open arrow) and surrounding epithelial crypt (solid arrow) of all teeth. Interestingly, there is also a progression of which teeth have odontoblasts where the pulp has acquired decreased volume, as the tooth matures. The teeth lower in the panel (red asterisks) have large pulp and represent replacement teeth that are just erupting, vs. the functional teeth where the odontoblasts surround a tooth with small pulp size. Correlating this pattern to *rspo3*

expression, it appears that *rspo3* labels replacement teeth pulp and odontoblasts whereas *col1a1* labels odontoblasts in all teeth. B) Higher magnification of single tooth cross-section indicating localized transcripts of *col1a1* in odontoblasts (open arrow) and in the epithelium (solid arrow) around the tooth (pulp marked with asterisk). In contrast, *rspo3* is more broadly expressed in dental pulp, odontoblasts (open arrow) and epithelial crypt surrounding the tooth (solid arrow). C) Sagittal section of teeth structure demonstrating *rspo3* and *col1a1* share expression in odontoblasts. However, *rspo3* has a broader and more diffuse expression that also includes the pulp cells (asterisk). Scale bar: 25 μm D) Detection of β-catenin activity using β-catenin immunohistochemistry in sagittal section of tooth structure. β-catenin is active in odontoblasts (open arrow), surrounding the pulp (asterisk) and crypt epithelium (solid arrow). Scale bar: 10 μm

Consistent with zebrafish results, *Rspo3* and *Col1a1* (odontoblast marker) are co-expressed in odontoblasts in the lower incisor and molars of mice at P7. Moreover, *Rspo3* is also more diffusely expressed in ameloblasts, dental pulp and alveolar bone (Fig. 20A,B,C). A summary of zebrafish teeth gene expression and the contribution of *rspo3* in bone and dental morphogenesis is shown in Fig. 21.

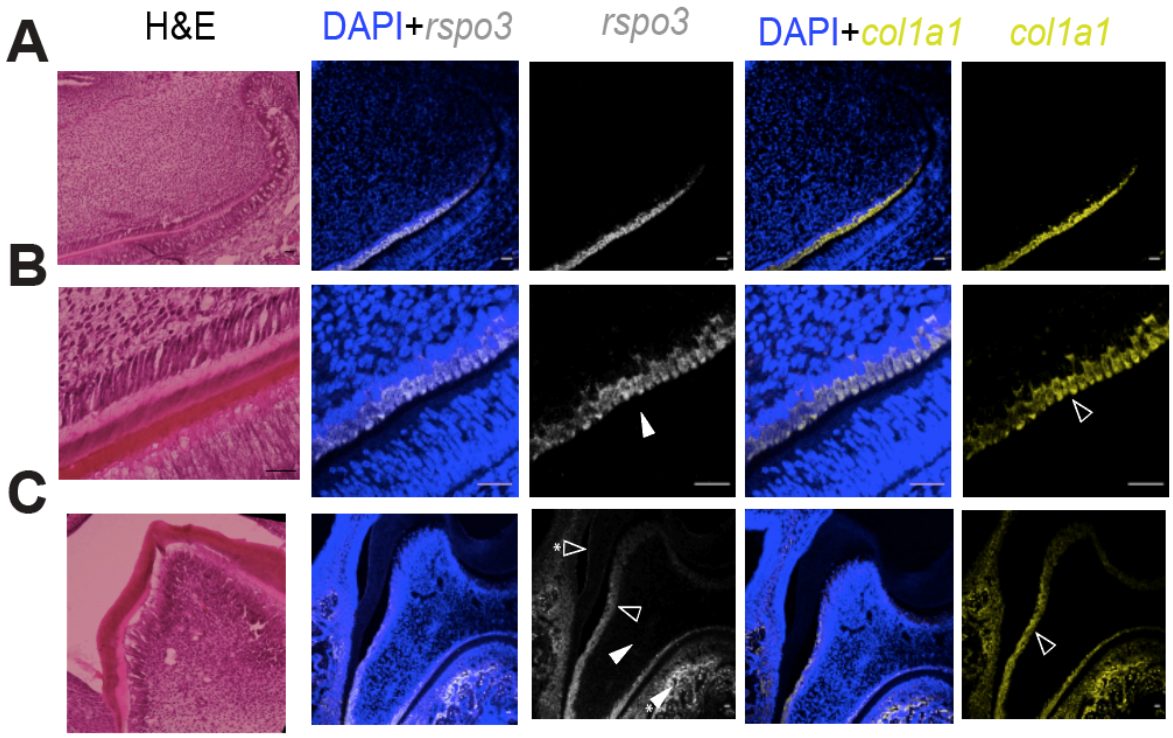

Fig. 20. Mouse teeth *rspo3* expression is similar to zebrafish teeth results. The H&E staining in A,B and C are different sections than the RNAscope sections. A) *Rspo3* and *Col1a1* are co-expressed in the odontoblasts in the lower incisor in mouse. B) Higher magnification of lower incisor cross-section showing *Col1a1* transcripts in odontoblasts (open arrow) and *Rspo3* is also expressed in odontoblasts (solid arrow). C) lower molar cross-section demonstrating co-expression of *Rspo3* and *Col1a1*

in odontoblasts (open arrow). In addition, *Rspo3* is expressed in the pulp (solid arrow) ameloblast (open arrow with asterisk) and alveolar bone (solid arrow with asterisk). Scale bar: 25 μm

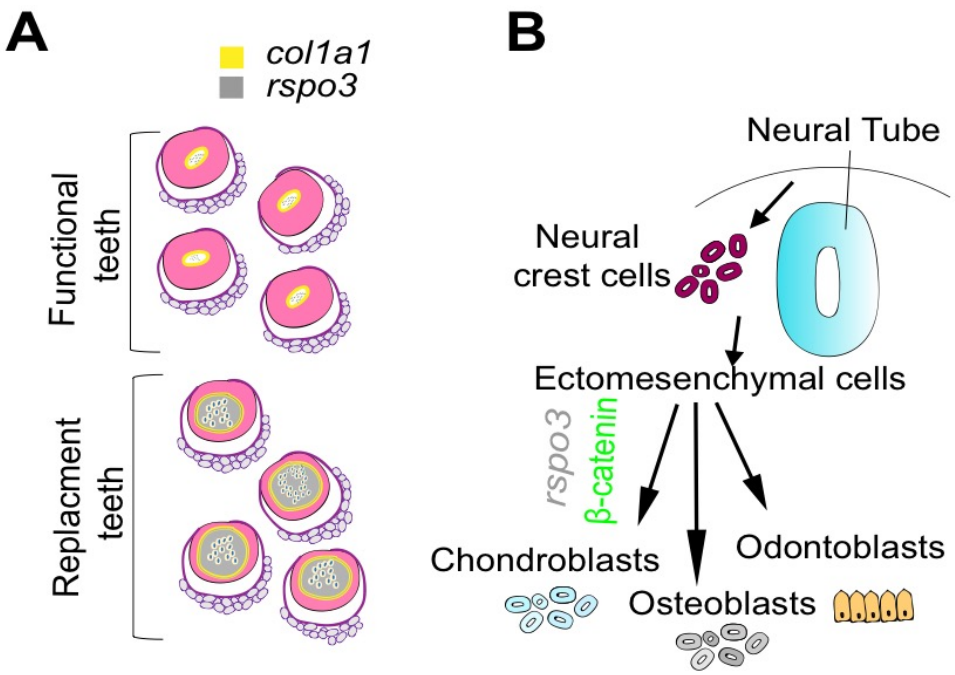

Fig. 21. Summary figure showing zebrafish dental gene expression and the role of *rspo3* in bone and teeth morphogenesis. A) Dental cross-sections are showing *rspo3* (gray) labels only replacement teeth pulp and odontoblast whereas *col1a1* (yellow) labels replacement and functional teeth odontoblasts in zebrafish. B) An important finding of this study is that *Rspo3* contribute to bone and dental morphogenesis.

Rspo3-/- zebrafish embryos exhibit reduced chondrogenesis maturation, and adults have decreased body length and midface deficiency.

To assess embryonic ossification initiation, whole mount Alizarin red staining was carried out at 10 dpf. We observed reduced ossification of maxillary, dentary, anguloarticular and ceraohyal bones in *rspo3*-/- mutants as compared to age matched wild type siblings (Fig. 22B). Moreover, whole mount Alcian and Alizarin staining showed absence of dentary bone ossification and malformed dentary cartilage in *rspo3*-/- mutants zebrafish at 7-9 dpf as

compared to wild type aged matched siblings (Fig. 22C). Interestingly, we also observed increased osteoclast activity in *rspo3-/-* mutants as revealed using TRAP staining (Fig. 23).

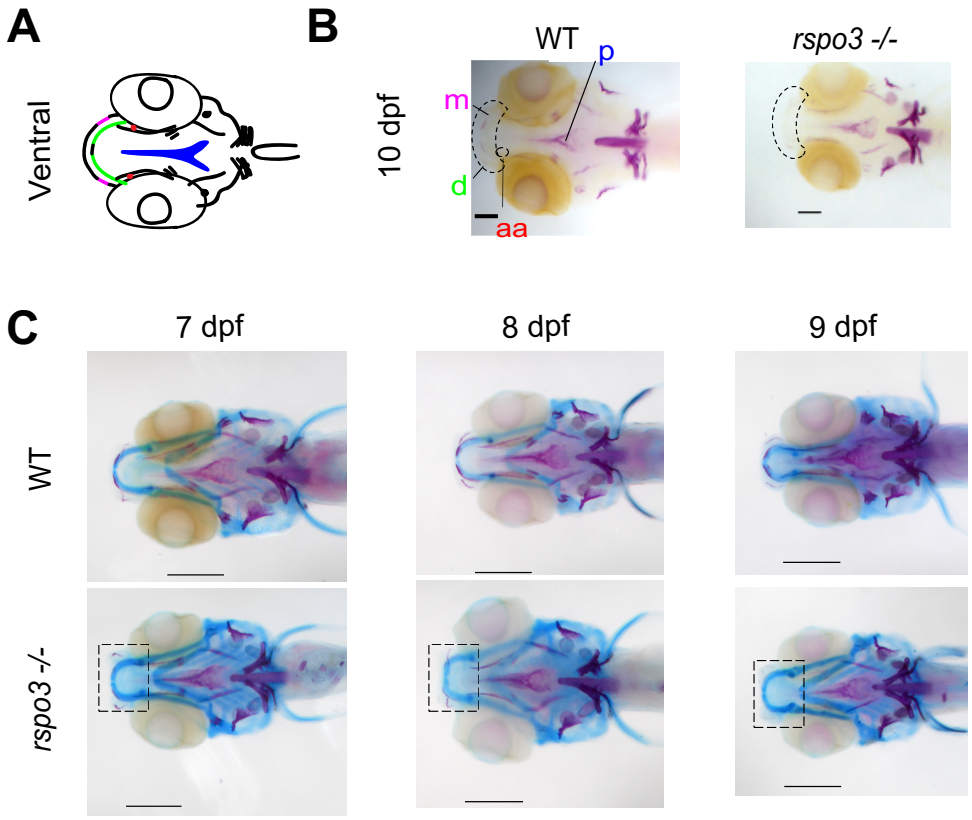

Fig. 22. Reduced ossification in *rspo3* mutants compared to wild type. Alizarin staining of 10 dpf embryo showing differences in craniofacial ossification in *rspo3* mutant in relation to wild type. A) Diagram of ventral view of 10 dpf embryo, with key cartilaginous elements labeled and color coded. B) Ventral views of Alizarin stained embryos at 10 dpf showing absence of maxilla (dotted outline), dentary bone ossification in the *rspo3-/-* mutant in relation to wild type fish. Abbreviations: aa: anguloarticular, d: dentary, m: maxilla, p: parashenoid. Scale bar: 10 μm. C) Ventral view of whole mount Alcian and Alizarin staining of 7-9 dpf zebrafish *rspo3-/-* mutants showing absences of dentary bone ossification and malformed dentary bone cartilage compared to wild type aged matched siblings. Scale bar: 25 μm.

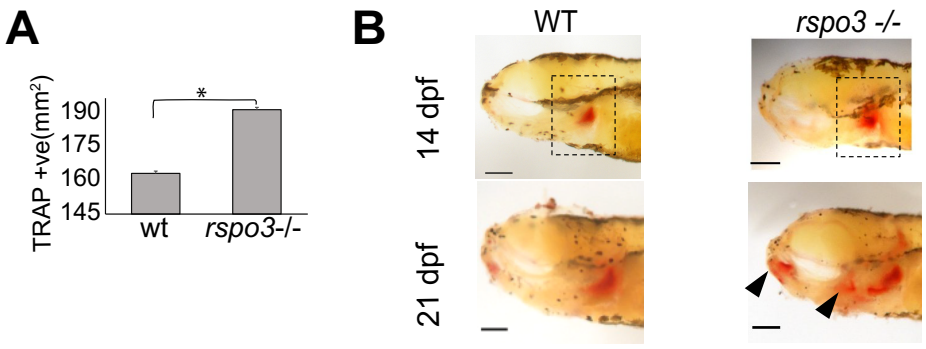

Fig. 23. **Increased osteoclast activity areas in *rspo3* mutants**. A) Significantly greater total TRAP positive areas in *rspo3*-/- mutants compared to wild type at 21 dpf. (*p ≤ 0.05). B) Lateral view of 14 dpf showing increase osteoclast activity (red stain in the black dotted box) in *rspo3* mutant compared to aged matched wild type. At 21 dpf, more areas of osteoclast activity in the dentary, hypomandibular, pharyngeal teeth and jaws (solid arrow) were observed in *rspo3*-/- compared to wild type. Scale bar: 10 μm.

As the *rspo3*-/- mutant zebrafish matured, we observed midface hypoplasia in adult zebrafish (180 dpf) in which supraethmoid and nasal bones were deficient (Fig. 24A). Statistically significant differences in body length (measured from the mouth opening to the base of the tail) were observed between wild type and *rspo3*-/- suggesting the importance of *rspo3* in total body growth (Fig. 24B). Furthermore, our data showed a significant decrease in parasphenoid and anguloarticular bone volume in *rspo3*-/- compared to age matched wild type siblings (Fig. 24C,D). Moreover, pronounced forehead and midface hypoplasia were noticed in the mutant. Therefore, we performed a quantitative analysis measuring the angle formed by the parasphenoid line and a line tangent to frontal bone in order to confirm the phenotype of frontal bossing. No statistically significant differences were found in *rspo3*-/- animal compared to wild type. On the other hand, midface deficiency was measured using the linear measurement from nasal bone to a line tangent to the frontal bone and dentary. Quantitative analysis showed statistically significant differences in the linear measurements between *rspo3*-/- and wild type

samples, indicating the presence of midface deficiency in the *rspo3-/-* mutant (Fig. 24E,F,G,H). Bone mineral density was also measured, but was not significantly different between *rspo3-/-* and aged matched wild type siblings.

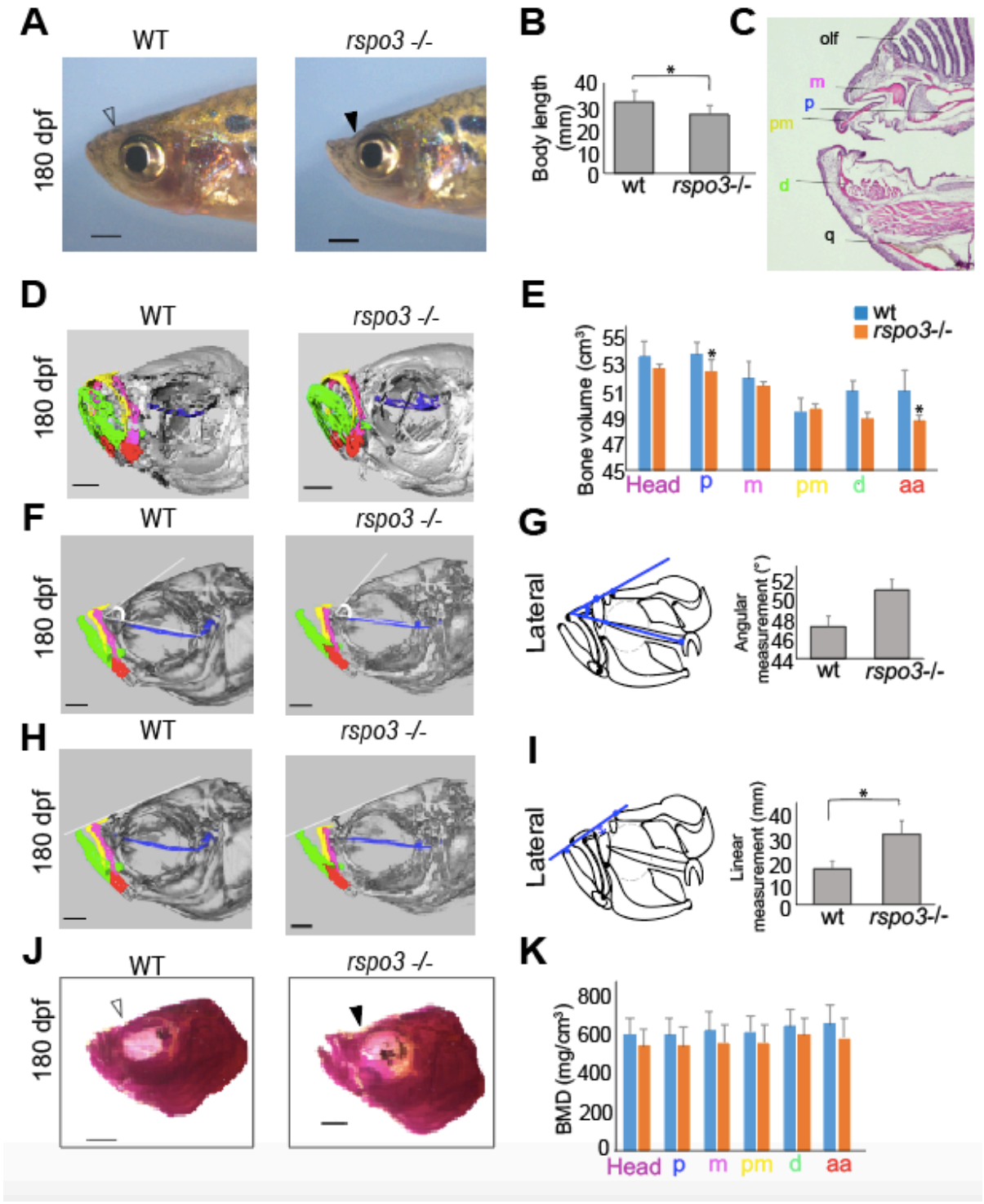

Fig. 24. Decreased body length and midface deficiency in *rspo3* mutants. A) Lateral images of *rspo3*-/- and wild type fish showing midface depression in *rspo3*-/- (solid arrow) in which the supraethmoid and nasal bones are deficient compared to wild type (open arrow). B) Bar chart showing statistically significant differences between wild type and *rspo3* -/- body length (measured from the tip of mouth opening to the base of the tail) using Student's t-test indicating *rspo3* importance in body growth (*p ≤ 0.05). C) H&E staining of sagittal section of adult fish (6 months old) demonstrating the bony landmarks; d:

dentary, m: maxilla, olf: olfactory, p: parashenoid, pm: premaxilla, q: quadrate. D) Oblique micro-CT image of *rspo3-/-* and wild type fish demonstrating color coded bone elements. E) Bar chart demonstrating the bone volume in the head and bone elements in *rspo3-/-* and wild type fish. Statistically significant difference was found in parasphenoid and anguloarticular bone volume which is less in *rspo3-/-* compared to wild type fish. Abbreviations: aa: anguloarticular, d: dentary, m: maxilla, p: parasphenoid, pm: premaxilla. Scale bar: 10 μm. F) 2D cephalometric analysis obtained from micro-CT of *rspo3-/-* and wild type fish. The angle formed by parasphenoid line and a line tangent to frontal bone identified frontal bossing, with increased angle in *rspo3-/-* compared to wild type. G) Diagram of lateral view of adult zebrafish showing the angular measurement. Bar chart showing no statistical differences in the angular measurement between *rspo3-/-* and wild type. H) 2D cephalometric analysis of *rspo3-/-* and wild type fish. The distance between nasal bone and a line drawn between dentary and frontal bone landmarks were measured in order to quantify midface depression in *rspo3-/-*. I) Diagram of lateral view of adult zebrafish showing the linear measurement from nasal bone to a line tangent to the frontal bone and dentary. The linear measurement value was significantly greater in *rspo3-/-* mutants than in wild type indicating the presence of midface hypoplasia ($*p \leq 0.05$). J) Alizarin staining of aged matched adult zebrafish (180 dpf) showed similar findings to the micro-Ct results. We found deficient midface in *rspo3-/-* (solid arrow) compared to wild type (open arrow). WT: wild type. Scale bar: 10 μm. K) Bar chart demonstrating the bone mineral density levels in the head and bone elements between *rspo3-/-* and wild type fish. No statistical significant difference was found in bone mineral density between *rspo3-/-* and wild type fish. BMD: bone mineral density.

rspo3 **is required for tooth morphogenesis.**

Analysis of dental morphology using micro-CT illustrated decreased tooth number and malalignment in *rspo3-/-* mutant zebrafish at 180 dpf, as compared to wild type aged matched siblings (Fig. 25A). In addition, whole mount Alizarin red staining showed malformed teeth at 7-9 dpf in the *rspo3-/-* mutant as compared to wild type siblings (Fig. 8B). At 180 dpf, we observed larger pulp and blunted tooth tips in the *rspo3-/-* mutant as compared to wild type siblings (Fig. 8B). Attached tooth number was significantly reduced in adult zebrafish *rspo3-/-* mutants as compared to wild type aged matched siblings, on both left and right pharyngeal

arches (Fig. 8C). These results underscore the importance of *rspo3* in dental development.

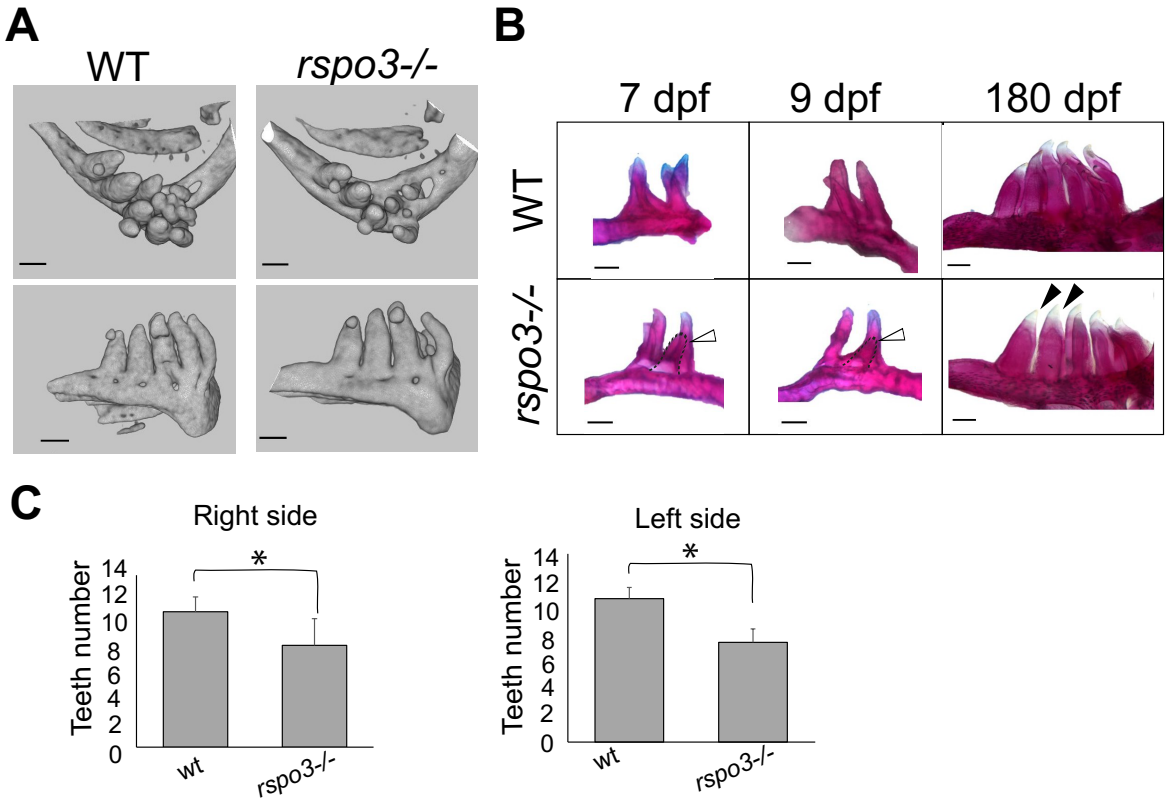

Fig. 25. Micro-CT imaging and Alizarin staining of adult zebrafish teeth (6 months old). A) Micro-CT reveals that the adult *rspo3*-/- animals exhibit hypodontia with several sockets missing teeth, the teeth that are present have longer crown and are malaligned compared to wild type. B) Alizarin red staining showing *rspo3*-/- mutant and wild type zebrafish teeth at three time points. At 7 dpf and 9 dpf, we observed malformed tooth (open arrow, dotted line), suggesting the hypodontia in *rspo3*-/- mutant zebrafish may be due to malformed and weaker tooth formation that leads to eventual tooth loss. At 180 dpf, staining revealed that the *rspo3*-/- mutant animals have blunted teeth tip (solid arrows) as compared to controls. Scale bar: 10 μm. C) Bar chart demonstrating the differences in teeth number between wild type and *rspo3*-/-. The Student's t-test showed statistically significant difference in teeth number between wild type and *rspo3*-/- in both sides (*$p \leq 0.05$).

Reduced odontoblast expression in *rspo3*-/- compared to wild type.

The decreased tooth number in *rspo3*-/- may be due to impaired tooth formation (Fig. 26). Therefore, RNAscope was performed to investigate odontoblasts in *rspo3*-/- compared to wild type fish. Our data showed less *col1a1* (odontoblast marker) in *rspo3*-/- compared to wild type fish (Fig. 26). Taken together, impairment of *rspo3* results in reduced odontoblast expression

which in turn affects dentin formation, making them more prone to rapid wear, breakage and tooth loss.

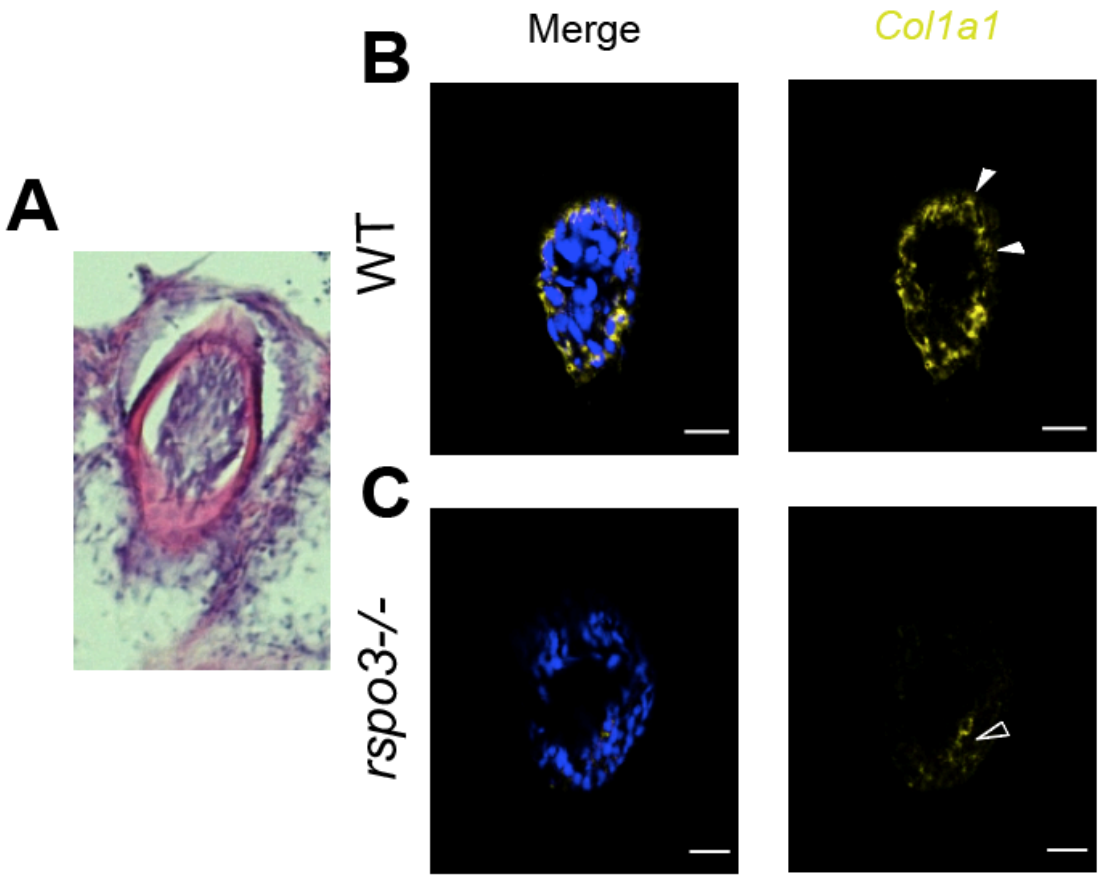

Fig. 26. CRISPR *rspo3* mutant zebrafish showed less dentin compared to wild type. The H&E staining in A is different section than the RNAscope sections. B) *col1a1* (odontoblast marker) is expressed in the odontoblasts in wild type zebrafish. C) *rspo3-/-* zebrafish showed less *col1a1* expression indicating less dentin formation. Scale bar: 15 μm

Discussion

Orofacial clefts are one of the most common congenital birth anomalies in humans, affecting 1 in 700 live births.[14] *IRF6* plays a major role in cleft pathogenesis, accounting for approximately 12%.[22,23] This study is based on the observation that *rspo3* was identified as a target gene for *irf6*. Our data demonstrated genetic and functional interaction between *irf6* and *rspo3.* Here, we analyzed *Rspo3* gene expression and function in craniofacial and dental morphogenesis, in zebrafish and mouse models. We showed that in zebrafish and mouse, *Rspo3* is expressed in perichondrial cells, but also at lower levels in *Runx2* positive osteoprogenitors in embryonic palate and Meckel's cartilage. In zebrafish teeth, *rspo3* is expressed in newly replacement teeth, and is broadly expressed in the pulp, odontoblasts, and crypt epithelium. In agreement with zebrafish teeth expression, *Rspo3* is expressed in odontoblasts, ameloblasts, pulp and alveolar bone in mouse lower incisor and molars. Gene knockdown of *rspo3* in the TCF/Lef:GFP reporter line confirmed that *rspo3* potentiates Wnt/β-catenin signaling in craniofacial bones. Analysis of *rspo3-/-* mutant embryos show that *rspo3* is required for initiation of osteogenesis in the maxilla, dentary bones, maintenance of bone density, and for adult teeth formation. Loss of *rspo3* resulted in delayed osteogenic initiation, exuberant osteoclast activity, midface hypoplasia, elongated dentary bone and reduced numbers of attached teeth in adult zebrafish, and dental malformation characterized by tooth crown tip blunting. These gene expression results and phenotypes are consistent with *rspo3* functioning in a progenitor cell population that is important for initiation craniofacial osteogenesis, formation and maintenance of bone and teeth.

Our data illustrated genetic and functional interaction between *irf6* and *rspo3*. The expression of *rspo3* was rescued by *irf6* mRNA injection into null *irf6* embryos, which indicates transcriptional activation of *rspo3* by *irf6* transcription.

In this study, we used RNAscope technology with a unique probe design that allows detection of mRNA by amplification of the signal and background suppression that leads to improved specificity.[93] We showed that high resolution gene expression analysis using RNAscope provided greater resolution in the case of cell types that are difficult to evaluate using whole mount approaches (compare Fig. 8 and Fig. 9). Since we hypothesized that *irf6* regulates *rspo3*, we expected that expression of these genes overlap during craniofacial development. At 24 hpf, co-expression of *irf6* and *rspo3* was detected in the zebrafish forebrain. Interestingly, neural crest cells in the forebrain have been reported to migrate and form oral epithelium.[5] This could suggest that *irf6* and *rspo3* contribute to the formation of oral epithelium later during development. We also found co-localization of *Irf6* and *Rspo3* transcripts in the first pharyngeal arch in zebrafish and mouse models. As mentioned earlier, the early pharyngeal arch patterning is conserved across vertebrates. In addition, the first pharyngeal arch contributes to the maxillary prominence that forms the lips and secondary palate, and the mandibular prominence the forms the lower jaw.[7] Therefore, *Irf6* and *Rspo3* play a role in craniofacial morphogenesis.

Using RNAscope, we were able to detect *rspo3* transcripts in cells that surround *sox10* expressing cells in palate trabeculae and in Meckel's cartilage. Moreover, *rspo3* is co-expressed with *Col1a1* (perichondrium marker) and *Runx2* (osteoprogenitor marker) in zebrafish and mice (Fig. 10). Similarly, a human genetic study has reported the involvement of *Rspo3* in bone mineral density and bone fractures.[31] Furthermore, *RSPO3* was reported to

regulate osteoblastic differentiation.[101] In addition, human *RSPO3* was identified as a candidate gene for cleft lip/palate and dental anomalies, consistent with its role in skeletal development in human adipose-derived stem cells.[58] Taken together, this and other studies corroborate the conclusion that *Rspo3* has conserved functions in the development of craniofacial bone and tooth structures across vertebrates.

Our findings are consistent with a previous study showing the same expression pattern of *rspo3* at the indicated embryonic stages using whole-mount *in situ* hybridization.[57] Knockdown of *rspo3* in zebrafish developed cardiac edema, small cranium, cleft palate and impaired lower jaw development. Similarly, *Xenopus* embryos with *rspo3* knockdown displayed cardiac edema due to vascular defects and small head cartilage.[62] In conjunction with previous studies[59], our data showed that *Rspo3* mutant mice at E10.5 die due to placental and vascular defects (Fig. 16). These results support the indications of our study that *rspo3* has a developmental role.

Our study included preliminary gene expression and knockdown studies to determine whether *rspo3* is expressed and functions in craniofacial cells. The specific expression of *rspo3* in the palate and Meckel's cartilage, and significant dysmorphology as a consequence of *rspo3* knockdown encouraged us to pursue a more detailed analysis (Fig. 15A). It is important to point out that the *rspo3-/-* embryonic phenotype is less severe than that observed with *rspo3*-MO knockdown (compare Fig. 13A and Fig. 15A). This difference in embryonic phenotype may be due to morpholino off-target effects making the morphant phenotype more severe, or gene compensation by other *rspo* family members, such as *rspo2*, in the CRISPR-Cas9 germline *rspo3* -20bp deletion allele. Similar to our findings, a recent article reported phenotypic differences between zebrafish knockouts and knockdowns, and proposed genetic

compensation in the knockouts but not in knockdown animals as a reason for the phenotypic differences.[102] In addition, *rspo2*-MO was injected in *rspo3*-/- and we observed a morphological phenotype characterized by a disrupted palate and Meckel's cartilage morphology and cardiac edema that could be masked by *rspo2* gene compensation (Fig. 15C). A previous study reported that knockdown of *upf1* in mutants lead to reduction of mRNA decay and thereafter loss of genetic adaptation.[100] For this reason, we also injected *upf1*-MO in *rspo3*-/- fish to eliminate transcriptional adaptation. Taken together, we found that the phenotype presented after injecting *rspo2*-MO and *upf1*-MO in *rspo3* -/- fish looked similar to the *rspo3*-MO phenotype, suggesting that *rspo2* compensation could be masking the *rspo3*-/- phenotype (Fig. 15C,D).

Another important finding is that *rspo3* regulates Wnt/β-catenin signaling during zebrafish development. Knockdown of *rspo3* decreased Wnt reporter activity in the ventral embryonic epithelium, which in turn leads to embryonic cartilage malformations. Consistent with our results, previous studies have reported that *rspo3* amplifies the Wnt/β-catenin pathway.[51,103,104] On the other hand, previous study also showed that *rspo3* knockdown leads to increased Wnt reporter signaling, indicating an inhibitory role for *rspo3* in the Wnt/β-catenin pathway.[57,105] Moreover, we investigated genetic interaction between *rspo3* and wnt genes such as *wls, wnt5b* and *gpc4.* We found that *wls* and *gpc4* expressions are induced in *rspo3*-MO fish, whereas *wnt5b* expression is reduced in *rspo3*-MO animals. Therefore, our results indicate that *rspo3* has an important role in the Wnt/β-catenin pathway and Wnt genes functions.

This study also identified a key requirement for *rspo3* in regulating tooth development. Zebrafish teeth are continuously replaced through life, where the regenerative process is

analogous to human adult tooth replacement of a deciduous, baby tooth and to continuously growing incisors in mice.[78,82,81] We found *rspo3* gene expression in dental pulp and odontoblasts in zebrafish and mice. This may suggest its involvement in the regulation of tooth development and dentinogenesis. Importantly, *rspo3* is preferentially detected in replacement teeth and absent in more mature teeth in zebrafish. Moreover, adult *rspo3-/-* zebrafish had decreased tooth number, abnormal morphology and abnormal orientation of teeth were abnormal compared to aged-matched wild type fish. Impairment of *rspo3* results in odontoblast reduction and deficient dentin formation, as shown in Fig. 26; this in turn affects dentin formation, making them more prone to rapid wear, breakage and tooth loss. Consistent with a previous report[106], β-catenin is expressed in odontoblasts, cells that constitute the epithelial crypt, inner and outer epithelium. Thus, Wnt/β-catenin signaling is important in tooth morphogenesis, and *rspo3* disruption inhibits dental development.[74]

As adults, *rspo3-/-* zebrafish developed midface hypoplasia, frontal bossing and reduction in tooth number and abnormal morphology compared to age-matched wild types zebrafish. Since our data showed co-expression of *rspo3* and *col1a1* in the perichondrium of Meckel's cartilage, the periosteum and the mandibular condyle during embryogenesis, these two genes could be functionally associated. Previous studies reported that patients with osteogenesis imperfecta caused by mutations in *COL1A1*, have frontal bossing, midface hypoplasia and dentinogenesis imperfecta.[98,99] Future studies to investigate *rspo3* molecular mechanism and its interaction with Wnt genes in regulating dental and bone development are recommended.

The clinical implication:

Orofacial cleft pathogenesis may be the result of a genetic predispositions influenced by environmental factors. *IRF6* is one of the most important genes implicated in orofacial clefts, in Van der Woude syndrome as well as non-syndromic orofacial cleft (OFC). We identified *Rspo3* as a transcriptional target of *Irf6*. We hypothesized that since *IRF6* is a key gene in regulating craniofacial development, investigations of *Rspo3* functions in the *Irf6* regulatory pathway provided additional mechanistic insights into the understand clinically relevant craniofacial biology that underlies OFC pathogenesis. Since *Rspo3* is a membrane protein[62], it is an efficient target for potential therapeutic drugs aimed at mitigating cleft lip and palate prenatally. Indeed, identification of *Irf6* targets is likely to result in improved prevention, treatment and prognosis of individuals with CL/P.

Limitation of the study:

In conjunction with previous studies[59], our data showed that *Rspo3* mutant mice at E10.5 die due to placental and vascular defects (Fig. 15). For this reason, we used conditional genetic mutations to identify the role of *Rspo3* in mice beyond E10.5. To identify neural crest-derived cell population, we crossed *Wnt1-Cre* mice with *Rspo3*$^{flox/flox}$ mice (Fig. 17). However, no phenotype was seen in *Wnt1-Cre*/+;*Rspo3*$^{flox/flox}$ mice. Although *Wnt1-Cre*-recombinase is highly efficient and results in ablation of approximately 96% of neural crest cells, this could be because *Wnt1* is not expressed in migratory neural crest cells.[107-110] Also, after neural crest delamination from the neural tube, *Wnt* activity decreases rapidly.[107-110] Therefore, it is difficult to investigate epithelial-to-mesenchymal transition or migration of neural crest cells using the *Wnt1-Cre* mouse line.[111]

Another limitation in this study is the non-successful characterization of *rspo3*-/- in zebrafish using western blot analysis. This might be due to low affinity of antibody to *rspo3* protein. In addition, wrong concentration of antibody could be the possible cause of Western analysis failure. Finally, antigen related problems such as not enough antigen loaded on the gel could be the cause. However, we have sequenced the *rspo3*-/- and found a frame shift and the introduction of premature stop codon.

Conclusions

Based on our data's findings, the following conclusions can be drawn:

- We discovered that *rspo3* genetically and functionally interact with *irf6* during craniofacial development.
- *Rspo3* is expressed in perichondrial cells that are juxtaposed to the oral epithelium and cartilage structures, chondrocytes, osteoprogenitor cells and oral epithelium.
- We show that *rspo3* function is required in a non-cell autonomous way to regulate osteogenesis of the chondrogenic cells, and that *rspo3* is also required for bone homeostasis.
- Canonical β-catenin mediated Wnt signaling activity is influenced by disruption of *rspo3* and our data showed genetic interaction between *rspo3* with Wnt genes such as *wls, wnt5b* and *gpc4*. Our study main findings are shown in Fig. 27.

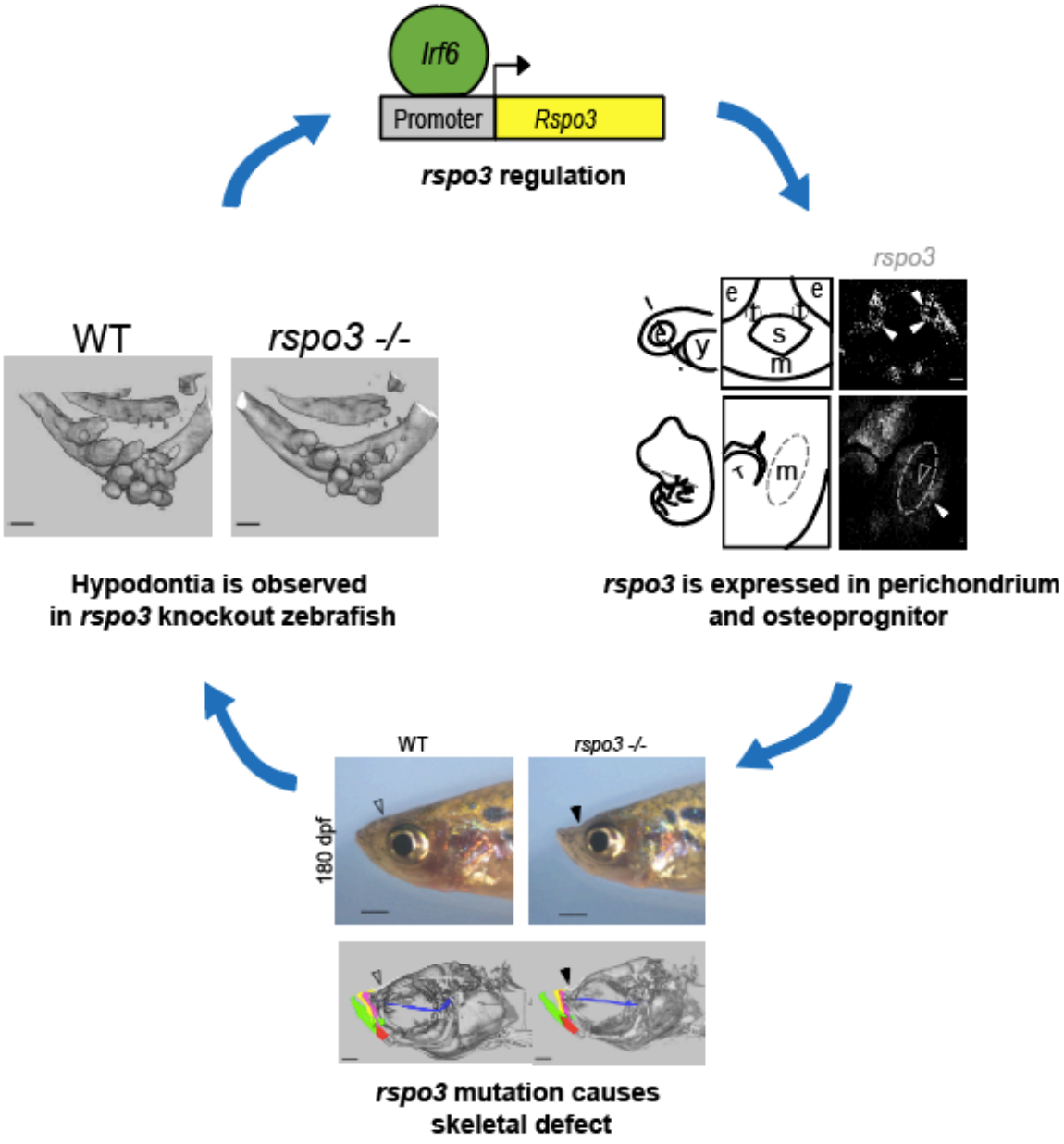

Fig 27. Summary of the study findings. *Rspo3* is regulated by *Irf6* during embryonic development. Also, *Rspo3* is expressed in perichondrium and osteoprogenitor cells. Adult zebrafish showed a skeletal phenotype characterized by midface hypoplasia. In addition, Adult zebrafish with *rspo3* knockout have less teeth compared to wild type.

References

1. Mao JJ, Nah H-D. Growth and development: hereditary and mechanical modulations. *American journal of orthodontics and dentofacial orthopedics.* 2004;125(6):676-689.
2. Vora S. Mouse models for the study of cranial base growth and anomalies. *Orthodontics & craniofacial research.* 2017;20:18-25.
3. Chai Y, Maxson RE. Recent advances in craniofacial morphogenesis. *Developmental Dynamics.* 2006;235(9):2353-2375.
4. Serbedzija GN, Bronner-Fraser M, Fraser SE. Vital dye analysis of cranial neural crest cell migration in the mouse embryo. *Development.* 1992;116(2):297-307.
5. Osumi-Yamashita N, Ninomiya Y, Eto K, Doi H. The contribution of both forebrain and midbrain crest cells to the mesenchyme in the frontonasal mass of mouse embryos. *Developmental biology.* 1994;164(2):409-419.
6. Larsen WJ. *Human embryology.* Churchill Livingstone; 2001.
7. Helms JA, Cordero D, Tapadia MD. New insights into craniofacial morphogenesis. *Development.* 2005;132(5):851-861.
8. Helms J, Schneider R. Cranial skeletal biology. *Nature.* 2003;423(6937):326.
9. Medeiros DM, Crump JG. New perspectives on pharyngeal dorsoventral patterning in development and evolution of the vertebrate jaw. *Developmental biology.* 2012;371(2):121-135.
10. Dougherty M, Kamel G, Grimaldi M, et al. Distinct requirements for wnt9a and irf6 in extension and integration mechanisms during zebrafish palate morphogenesis. *Development.* 2013;140(1):76-81.
11. Wada N, Javidan Y, Nelson S, Carney TJ, Kelsh RN, Schilling TF. Hedgehog signaling is required for cranial neural crest morphogenesis and chondrogenesis at the midline in the zebrafish skull. *Development.* 2005;132(17):3977-3988.
12. Mork L, Crump G. Zebrafish craniofacial development: a window into early patterning. In: *Current topics in developmental biology.* Vol 115. Elsevier; 2015:235-269.
13. Van Otterloo E, Williams T, Artinger KB. The old and new face of craniofacial research: how animal models inform human craniofacial genetic and clinical data. *Developmental biology.* 2016;415(2):171-187.
14. Moosey P, Little J. Epidemiology of oral clefts: An international perspective In: Wyszynski DF, editor Cleft lip and palate: From origin to treatment. In: Oxford: Oxford University Press; 2002.
15. Rahimov F, Jugessur A, Murray JC. Genetics of nonsyndromic orofacial clefts. *Cleft Palate Craniofac J.* 2012;49(1):73-91.
16. Jugessur A, Murray JC. Orofacial clefting: recent insights into a complex trait. *Current opinion in genetics & development.* 2005;15(3):270-278.
17. Lidral AC, Moreno LM. Progress toward discerning the genetics of cleft lip. *Current opinion in pediatrics.* 2005;17(6):731.
18. Habel A, Sell D, Mars M. Management of cleft lip and palate. *Archives of disease in childhood.* 1996;74(4):360-366.

19. Jugessur A, Farlie P, Kilpatrick N. The genetics of isolated orofacial clefts: from genotypes to subphenotypes. *Oral diseases.* 2009;15(7):437-453.
20. Washbourne BJ, Cox TC. Expression profiles of cIRF6, cLHX6 and cLHX7 in the facial primordia suggest specific roles during primary palatogenesis. *BMC developmental biology.* 2006;6(1):18.
21. Kondo S, Schutte BC, Richardson RJ, et al. Mutations in IRF6 cause Van der Woude and popliteal pterygium syndromes. *Nature genetics.* 2002;32(2):285.
22. Jugessur A, Rahimov F, Lie RT, et al. Genetic variants in IRF6 and the risk of facial clefts: single‐marker and haplotype‐based analyses in a population‐based case‐control study of facial clefts in Norway. *Genetic epidemiology.* 2008;32(5):413-424.
23. Zucchero TM, Cooper ME, Maher BS, et al. Interferon regulatory factor 6 (IRF6) gene variants and the risk of isolated cleft lip or palate. *New England Journal of Medicine.* 2004;351(8):769-780.
24. Beaty TH, Murray JC, Marazita ML, et al. A genome-wide association study of cleft lip with and without cleft palate identifies risk variants near MAFB and ABCA4. *Nature genetics.* 2010;42(6):525.
25. Ben J, Jabs EW, Chong SS. Genomic, cDNA and embryonic expression analysis of zebrafish IRF6, the gene mutated in the human oral clefting disorders Van der Woude and popliteal pterygium syndromes. *Gene Expr Patterns.* 2005;5(5):629-638.
26. Ferretti E, Li B, Zewdu R, et al. A conserved Pbx-Wnt-p63-Irf6 regulatory module controls face morphogenesis by promoting epithelial apoptosis. *Developmental cell.* 2011;21(4):627-641.
27. Iwata J-i, Suzuki A, Pelikan RC, et al. Smad4-Irf6 genetic interaction and TGF_-mediated IRF6 signaling cascade are crucial for palatal fusion in mice. *Development.* 2013:dev. 089615.
28. Gavin BJ, McMahon JA, McMahon AP. Expression of multiple novel Wnt-1/int-1-related genes during fetal and adult mouse development. *Genes & development.* 1990;4(12b):2319-2332.
29. Brault V, Moore R, Kutsch S, et al. Inactivation of the (β)-catenin gene by Wnt1-Cre-mediated deletion results in dramatic brain malformation and failure of craniofacial development. *Development.* 2001;128(8):1253-1264.
30. Cadigan KM, Nusse R. Wnt signaling: a common theme in animal development. *Genes & development.* 1997;11(24):3286-3305.
31. Brugmann SA, Goodnough LH, Gregorieff A, et al. Wnt signaling mediates regional specification in the vertebrate face. *Development.* 2007;134(18):3283-3295.
32. Vendrell V, Summerhurst K, Sharpe J, Davidson D, Murphy P. Gene expression analysis of canonical Wnt pathway transcriptional regulators during early morphogenesis of the facial region in the mouse embryo. *Gene Expression Patterns.* 2009;9(5):296-305.
33. Geetha‐Loganathan P, Nimmagadda S, Antoni L, et al. Expression of WNT signalling pathway genes during chicken craniofacial development. *Developmental Dynamics.* 2009;238(5):1150-1165.

34. Sisson BE, Topczewski J. Expression of five frizzleds during zebrafish craniofacial development. *Gene Expression Patterns.* 2009;9(7):520-527.
35. Niemann S, Zhao C, Pascu F, et al. Homozygous WNT3 mutation causes tetra-amelia in a large consanguineous family. *The American Journal of Human Genetics.* 2004;74(3):558-563.
36. Little RD, Folz C, Manning SP, et al. A mutation in the LDL receptor–related protein 5 gene results in the autosomal dominant high–bone-mass trait. *The American Journal of Human Genetics.* 2002;70(1):11-19.
37. Boyden LM, Mao J, Belsky J, et al. High bone density due to a mutation in LDL-receptor–related protein 5. *New England Journal of Medicine.* 2002;346(20):1513-1521.
38. Baron R, Kneissel M. WNT signaling in bone homeostasis and disease: from human mutations to treatments. *Nature medicine.* 2013;19(2):179.
39. Glass II DA, Karsenty G. Molecular bases of the regulation of bone remodeling by the canonical Wnt signaling pathway. *Current topics in developmental biology.* 2006;73:43-84.
40. Albers J, Keller J, Baranowsky A, et al. Canonical Wnt signaling inhibits osteoclastogenesis independent of osteoprotegerin. *J Cell Biol.* 2013;200(4):537-549.
41. Kim K-A, Zhao J, Andarmani S, et al. R-Spondin proteins: a novel link to β-catenin activation. *Cell cycle.* 2006;5(1):23-26.
42. Cruciat C-M, Niehrs C. Secreted and transmembrane wnt inhibitors and activators. *Cold Spring Harbor perspectives in biology.* 2013;5(3):a015081.
43. Hao H-X, Xie Y, Zhang Y, et al. ZNRF3 promotes Wnt receptor turnover in an R-spondin-sensitive manner. *Nature.* 2012;485(7397):195.
44. Koo B-K, Spit M, Jordens I, et al. Tumour suppressor RNF43 is a stem-cell E3 ligase that induces endocytosis of Wnt receptors. *Nature.* 2012;488(7413):665.
45. Lebensohn AM, Rohatgi R. R-spondins can potentiate WNT signaling without LGRs. *eLife.* 2018;7:e33126.
46. Kazanskaya O, Glinka A, del Barco Barrantes I, Stannek P, Niehrs C, Wu W. R-Spondin2 is a secreted activator of Wnt/β-catenin signaling and is required for Xenopus myogenesis. *Developmental cell.* 2004;7(4):525-534.
47. Aoki M, Kiyonari H, Nakamura H, Okamoto H. R-spondin2 expression in the apical ectodermal ridge is essential for outgrowth and patterning in mouse limb development. *Dev Growth Differ.* 2008;50(2):85-95.
48. Parma P, Radi O, Vidal V, et al. R-spondin1 is essential in sex determination, skin differentiation and malignancy. *Nature genetics.* 2006;38(11):1304.
49. Baran R, Kechijian P. Understanding nail disorders. *European journal of dermatology: EJD.* 2001;11(2):159-162.
50. Blaydon DC, Ishii Y, O'Toole EA, et al. The gene encoding R-spondin 4 (RSPO4), a secreted protein implicated in Wnt signaling, is mutated in inherited anonychia. *Nature genetics.* 2006;38(11):1245.
51. Kim K-A, Wagle M, Tran K, et al. R-Spondin family members regulate the Wnt pathway by a common mechanism. *Molecular biology of the cell.* 2008;19(6):2588-2596.

52. Jin Y-R, Turcotte TJ, Crocker AL, Han XH, Yoon JK. The canonical Wnt signaling activator, R-spondin2, regulates craniofacial patterning and morphogenesis within the branchial arch through ectodermal–mesenchymal interaction. *Developmental biology.* 2011;352(1):1-13.
53. Szenker-Ravi E, Altunoglu U, Leushacke M, et al. RSPO2 inhibition of RNF43 and ZNRF3 governs limb development independently of LGR4/5/6. *Nature.* 2018;557(7706):564-569.
54. Bell SM, Schreiner CM, Wert SE, Mucenski ML, Scott WJ, Whitsett JA. R-spondin 2 is required for normal laryngeal-tracheal, lung and limb morphogenesis. *Development.* 2008;135(6):1049-1058.
55. Yamada W, Nagao K, Horikoshi K, et al. Craniofacial malformation in R-spondin2 knockout mice. *Biochemical and biophysical research communications.* 2009;381(3):453-458.
56. Baenziger NL, Brodie G, Majerus PW. A thrombin-sensitive protein of human platelet membranes. *Proceedings of the National Academy of Sciences.* 1971;68(1):240-243.
57. Rong X, Chen C, Zhou P, et al. R-spondin 3 regulates dorsoventral and anteroposterior patterning by antagonizing Wnt/β-catenin signaling in zebrafish embryos. *PLoS One.* 2014;9(6):e99514.
58. Vieira AR, McHenry TG, Daack-Hirsch S, Murray JC, Marazita ML. Candidate gene/loci studies in cleft lip/palate and dental anomalies finds novel susceptibility genes for clefts. *Genetics in Medicine.* 2008;10(9):668.
59. Aoki M, Mieda M, Ikeda T, Hamada Y, Nakamura H, Okamoto H. R-spondin3 is required for mouse placental development. *Developmental biology.* 2007;301(1):218-226.
60. Kazanskaya O, Ohkawara B, Heroult M, et al. The Wnt signaling regulator R-spondin 3 promotes angioblast and vascular development. *Development.* 2008;135(22):3655-3664.
61. Neufeld S, Rosin JM, Ambasta A, et al. A conditional allele of Rspo3 reveals redundant function of R‐spondins during mouse limb development. *genesis.* 2012;50(10):741-749.
62. Ohkawara B, Glinka A, Niehrs C. Rspo3 binds syndecan 4 and induces Wnt/PCP signaling via clathrin-mediated endocytosis to promote morphogenesis. *Developmental cell.* 2011;20(3):303-314.
63. Jin Y-R, Yoon JK. The R-spondin family of proteins: emerging regulators of WNT signaling. *The international journal of biochemistry & cell biology.* 2012;44(12):2278-2287.
64. Knight MN, Karuppaiah K, Lowe M, et al. R-spondin-2 is a Wnt agonist that regulates osteoblast activity and bone mass. *Bone research.* 2018;6(1):24.
65. Correa‐Rodríguez M, Schmidt Rio‐Valle J, Rueda‐Medina B. The RSPO3 gene as genetic markers for bone mass assessed by quantitative ultrasound in a population of young adults. *Annals of human genetics.* 2018;82(3):143-149.
66. Knight MN, Hankenson KD. R-spondins: novel matricellular regulators of the skeleton. *Matrix Biology.* 2014;37:157-161.

67. Moayyeri A, Hsu Y-H, Karasik D, et al. Genetic determinants of heel bone properties: genome-wide association meta-analysis and replication in the GEFOS/GENOMOS consortium. *Human molecular genetics.* 2014;23(11):3054-3068.
68. Luo J, Yang Z, Ma Y, et al. LGR4 is a receptor for RANKL and negatively regulates osteoclast differentiation and bone resorption. *Nature medicine.* 2016;22(5):539.
69. Hankenson KD, Sweetwyne MT, Shitaye H, Posey KL. Thrombospondins and novel TSR-containing proteins, R-spondins, regulate bone formation and remodeling. *Current osteoporosis reports.* 2010;8(2):68-76.
70. Nam J-S, Turcotte TJ, Yoon JK. Dynamic expression of R-spondin family genes in mouse development. *Gene Expression Patterns.* 2007;7(3):306-312.
71. Liu H, Leslie EJ, Jia Z, et al. Irf6 directly regulates Klf17 in zebrafish periderm and Klf4 in murine oral epithelium, and dominant-negative KLF4 variants are present in patients with cleft lip and palate. *Human molecular genetics.* 2016;25(4):766-776.
72. Liu F, Millar SE. Wnt/β-catenin signaling in oral tissue development and disease. *Journal of dental research.* 2010;89(4):318-330.
73. Thesleff I. Epithelial-mesenchymal signalling regulating tooth morphogenesis. *Journal of cell science.* 2003;116(9):1647-1648.
74. Liu F, Chu EY, Watt B, et al. Wnt/β-catenin signaling directs multiple stages of tooth morphogenesis. *Developmental biology.* 2008;313(1):210-224.
75. Borday‐Birraux V, Van der Heyden C, Debiais‐Thibaud M, et al. Expression of Dlx genes during the development of the zebrafish pharyngeal dentition: evolutionary implications. *Evolution & development.* 2006;8(2):130-141.
76. Stock DW. Zebrafish dentition in comparative context. *Journal of Experimental Zoology Part B: Molecular and Developmental Evolution.* 2007;308(5):523-549.
77. Stock DW. The genetic basis of modularity in the development and evolution of the vertebrate dentition. *Philosophical Transactions of the Royal Society of London Series B: Biological Sciences.* 2001;356(1414):1633-1653.
78. Cobourne MT, Sharpe PT. Making up the numbers: The molecular control of mammalian dental formula. Paper presented at: Seminars in cell & developmental biology2010.
79. Kuang‐Hsien Hu J, Mushegyan V, Klein OD. On the cutting edge of organ renewal: Identification, regulation, and evolution of incisor stem cells. *genesis.* 2014;52(2):79-92.
80. Tucker A, Sharpe P. The cutting-edge of mammalian development; how the embryo makes teeth. *Nature Reviews Genetics.* 2004;5(7):499.
81. Tummers M, Thesleff I. Root or crown: a developmental choice orchestrated by the differential regulation of the epithelial stem cell niche in the tooth of two rodent species. *Development.* 2003;130(6):1049-1057.
82. Yelick PC, Schilling TF. Molecular dissection of craniofacial development using zebrafish. *Critical Reviews in Oral Biology & Medicine.* 2002;13(4):308-322.
83. Van der heyden C, Huysseune A. Dynamics of tooth formation and replacement in the zebrafish (Danio rerio)(Teleostei, Cyprinidae). *Developmental dynamics:*

an official publication of the American Association of Anatomists. 2000;219(4):486-496.
84. Kimmel CB, Ballard WW, Kimmel SR, Ullmann B, Schilling TF. Stages of embryonic development of the zebrafish. *Developmental dynamics.* 1995;203(3):253-310.
85. Shimizu N, Kawakami K, Ishitani T. Visualization and exploration of Tcf/Lef function using a highly responsive Wnt/β-catenin signaling-reporter transgenic zebrafish. *Developmental biology.* 2012;370(1):71-85.
86. Ling IT, Rochard L, Liao EC. Distinct requirements of wls, wnt9a, wnt5b and gpc4 in regulating chondrocyte maturation and timing of endochondral ossification. *Developmental biology.* 2017;421(2):219-232.
87. Walker M, Kimmel C. A two-color acid-free cartilage and bone stain for zebrafish larvae. *Biotechnic & Histochemistry.* 2007;82(1):23-28.
88. Aceto J, Nourizadeh-Lillabadi R, Marée R, et al. Zebrafish bone and general physiology are differently affected by hormones or changes in gravity. *PloS one.* 2015;10(6):e0126928.
89. Harris MP, Rohner N, Schwarz H, Perathoner S, Konstantinidis P, Nüsslein-Volhard C. Zebrafish eda and edar mutants reveal conserved and ancestral roles of ectodysplasin signaling in vertebrates. *PLoS genetics.* 2008;4(10).
90. Hammond CL, Schulte-Merker S. Two populations of endochondral osteoblasts with differential sensitivity to Hedgehog signalling. *Development.* 2009;136(23):3991-4000.
91. Copper JE, Budgeon LR, Foutz CA, et al. Comparative analysis of fixation and embedding techniques for optimized histological preparation of zebrafish. *Comparative Biochemistry and Physiology Part C: Toxicology & Pharmacology.* 2018;208:38-46.
92. Charles JF, Sury M, Tsang K, et al. Utility of quantitative micro-computed tomographic analysis in zebrafish to define gene function during skeletogenesis. *Bone.* 2017;101:162-171.
93. Wang F, Flanagan J, Su N, et al. RNAscope: a novel in situ RNA analysis platform for formalin-fixed, paraffin-embedded tissues. *The Journal of Molecular Diagnostics.* 2012;14(1):22-29.
94. Cheng R-K, Jesuthasan SJ, Penney TB. Zebrafish forebrain and temporal conditioning. *Philosophical Transactions of the Royal Society B: Biological Sciences.* 2014;369(1637):20120462.
95. Ma D, Wang X, Guo J, Zhang J, Cai T. Identification of a novel mutation of RUNX2 in a family with supernumerary teeth and craniofacial dysplasia by whole-exome sequencing: A case report and literature review. *Medicine.* 2018;97(32):e11328.
96. Zou L, Kidwai FK, Kopher RA, et al. Use of RUNX2 expression to identify osteogenic progenitor cells derived from human embryonic stem cells. *Stem cell reports.* 2015;4(2):190-198.
97. Baniwal SK, Shah PK, Shi Y, et al. Runx2 promotes both osteoblastogenesis and novel osteoclastogenic signals in ST2 mesenchymal progenitor cells. *Osteoporosis international : a journal established as result of cooperation between the European Foundation for Osteoporosis and the National Osteoporosis Foundation of the USA.* 2012;23(4):1399-1413.

98. da Fontoura CG, Miller S, Wehby G, et al. Candidate gene analyses of skeletal variation in malocclusion. *Journal of dental research.* 2015;94(7):913-920.
99. Pallos D, Hart P, Cortelli JR, et al. Novel COL1A1 mutation (G599C) associated with mild osteogenesis imperfecta and dentinogenesis imperfecta. *Archives of Oral Biology.* 2001;46(5):459-470.
100. El-Brolosy MA, Kontarakis Z, Rossi A, et al. Genetic compensation triggered by mutant mRNA degradation. *Nature.* 2019;568(7751):193.
101. Zhang M, Zhang P, Liu Y, et al. RSPO3-LGR4 regulates osteogenic differentiation of human adipose-derived stem cells via ERK/FGF signalling. *Scientific reports.* 2017;7:42841.
102. Rossi A, Kontarakis Z, Gerri C, et al. Genetic compensation induced by deleterious mutations but not gene knockdowns. *Nature.* 2015;524(7564):230.
103. Nam J-S, Turcotte TJ, Smith PF, Choi S, Yoon JK. Mouse cristin/R-spondin family proteins are novel ligands for the Frizzled 8 and LRP6 receptors and activate β-catenin-dependent gene expression. *Journal of Biological Chemistry.* 2006;281(19):13247-13257.
104. Glinka A, Dolde C, Kirsch N, et al. LGR4 and LGR5 are R‐spondin receptors mediating Wnt/ β ‐catenin and Wnt/PCP signalling. *EMBO reports.* 2011;12(10):1055-1061.
105. Maes C, Bouillon R, Martin TJ. The first IBMS Herbert Fleisch Workshop. *BoneKEy Reports.* 2014;11.
106. Verstraeten B, van Hengel J, Huysseune A. Beta-catenin and plakoglobin expression during zebrafish tooth development and replacement. *PloS one.* 2016;11(3):e0148114.
107. Kléber M, Lee H-Y, Wurdak H, et al. Neural crest stem cell maintenance by combinatorial Wnt and BMP signaling. *The Journal of cell biology.* 2005;169(2):309-320.
108. Hari L, Miescher I, Shakhova O, et al. Temporal control of neural crest lineage generation by Wnt/β-catenin signaling. *Development.* 2012;139(12):2107-2117.
109. Rabadán MA, Herrera A, Fanlo L, et al. Delamination of neural crest cells requires transient and reversible Wnt inhibition mediated by Dact1/2. *Development.* 2016;143(12):2194-2205.
110. Zervas M, Millet S, Ahn S, Joyner AL. Cell behaviors and genetic lineages of the mesencephalon and rhombomere 1. *Neuron.* 2004;43(3):345-357.
111. Debbache J, Parfejevs V, Sommer L. Cre‐driver lines used for genetic fate mapping of neural crest cells in the mouse: An overview. *genesis.* 2018;56(6-7):e23105.